REVIEWS



Multiphase flow behaviour and hazard prediction of pyroclastic density currents

Gert Lube¹ ¹ [∞], Eric C. P. Breard², Tomaso Esposti-Ongaro³, Josef Dufek² and Brittany Brand⁴

Abstract | Pyroclastic density currents (PDCs) are dangerous multiphase flows originating from volcanic eruptions. PDCs cause more than a third of volcanic fatalities globally and, therefore, development of robust PDC hazard models is a priority in volcanology and natural hazard science. However, the complexity of gas—particle interactions inside PDCs, as well as their hostile nature, makes quantitative measurements of internal flow properties, and the validation of hazard models, challenging. Within the last decade, major advances from large-scale experiments, field observations and computational and theoretical models have provided new insights into the enigmatic internal structure of PDCs and identified key processes behind their fluid-like motion. Recent developments have also revealed important links between newly recognized processes of mesoscale turbulence and PDC behaviour. In this Review, we consider how recent advances in PDC research close the gaps towards more robust hazard modelling, outline the need to measure the internal properties of natural flows using geophysical methods and identify critical future research challenges. Greater understanding of PDCs will also provide insights into the dynamics of other natural gravity currents and high-energy turbulent multiphase flows, such as debris avalanches and turbidity currents.

Gravity currents

When a fluid of one density propagates into a different fluid of contrasting density.

Hazard footprints

The area impacted by one or more hazard(s).

¹Institute of Geosciences, Massey University, Palmerston North, New Zealand.

²Department of Earth Sciences, University of Oregon, Eugene, OR, USA.

³Istituto Nazionale di Geofisica e Vulcanologia – Sezione di Pisa, Pisa, Italy.

⁴Department of Geosciences, Boise State University, Boise,

⊠e-mail: g.lube@massey.ac.nz https://doi.org/10.1038/s43017-020-0064-8

Pyroclastic density currents (PDCs) represent one of the most dangerous and least understood phenomena of explosive volcanism. PDCs form when hot mixtures of volcanic ash, rock and gas fail to become positively buoyant (with respect to air) and develop ground-hugging gravity currents that entrain, and laterally intrude into, the colder and less dense atmosphere (FIG. 1a). Many volcanic systems worldwide, which display a range of eruptive styles and magnitudes, are associated with frequent PDCs¹, demonstrating that these flows are associated with a wide spectrum of eruption processes, such as collapse of eruptive plumes²,3 and lava domes⁴,5, directed magmatic⁶,7 and hydrothermal blasts®,9, phreatic and phreatomagmatic explosions¹0,11, and caldera-collapse events¹2,13.

The impacts of PDCs are determined by their high velocities and mobility, resulting in large and uncertain hazard footprints^{14–17}; high dynamic pressure, causing partial to complete destruction to the built environment around volcanoes^{18–20}; and their abundance of very fine and hot ash particles, causing asphyxiation and burn risks^{21,22}. In the last decade, the number of confirmed fatalities from PDC-forming eruptions of Merapi (Indonesia) in 2010 (REF.²³), Ontake (Japan) in 2014

(REF.¹⁰), Sinabung (Indonesia) in 2014 (REF.²⁴) and 2016 (REFS^{25,26}), Fuego (Guatemala) in 2018 (REF.²⁷), Stromboli (Italy) in 2019 and White Island (New Zealand) in 2019 totals at least 650 people. The number of fatalities would have been much higher if, for example, geophysical monitoring in 2010 had not called for a timely mass evacuation at Merapi²⁸ or if the mobile-blast-like PDCs of the 2012 Te Maari eruption had engulfed New Zealand's most popular hiking track during daytime⁸. Nevertheless, PDCs account for one-third of volcanic fatalities and injuries globally²⁹, and multiple disasters in the last decade raise concerns about the ability to mitigate PDC hazards.

Overall, nearly 100 million people now live at risk from PDCs^{20,31}, demonstrating why the development of robust hazard modelling and PDC risk-mitigation strategies are essential. Hazard modelling, however, depends on understanding the physical processes that control PDCs, which constitutes a primary research objective in physical volcanology and volcanic hazard sciences.

Investigating the physical processes that operate within PDCs is impeded by three main challenges. First, PDCs are one of the most complex types of natural multiphase flow. The fluid and thermodynamic behaviour of

Key points

- We are not yet learning quickly enough about pyroclastic density currents (PDCs) to save lives.
- Recent advances in experimental and computational studies delineate the concentration boundaries that separate dilute, intermediate and concentrated regimes of PDC transport.
- Mass and momentum transfer between dilute and concentrated flow regions, and, thus, the evolving transport behaviour, is controlled by the recently identified intermediate regime.
- Identification of pore-pressure feedbacks in experimental PDCs, combined with multiphase modelling, provide insights into the origin of the high mobility and extremely low effective friction of PDCs.
- New geophysical methods to probe the internal flow structure are becoming available and will provide data to test existing PDC flow models and drive future research.
- The advanced understanding of PDCs gained from combining experimental, computational and field approaches must be used to benchmark, validate and advance PDC hazard models.

PDCs includes concurrent particle-particle and fluidparticle interactions, fluid shear, turbulent fluctuations, and entrainment and mixing of ambient air. The importance of each process is governed by broad and overlapping characteristic length scales and timescales (FIG. 1b), which leads to a wide spectrum of possible, concurrent flow regimes, including compressible turbulent flow, gas pore-pressure-modified granular flow and dry granular flow. Based on the characteristics of PDC deposits, volcanologists have traditionally distinguished two types of PDCs: pyroclastic flows and pyroclastic surges. Flows and surges are often viewed as endmembers of PDC behaviour, which are dominated by gas-particle transport at high or low particle volume concentration, respectively (FIG. 1a). However, understanding of the multiscale and multiphase processes that develop across the spectrum of dynamic flow regimes in PDCs remains incomplete³².

Second, direct observations and measurements of the internal structure of PDCs, which could be used to clarify and characterize the complex array of processes operating within them, remain rare and are limited by the hostile nature of these flows. In addition, the paucity of direct geophysical observations means that estimates of the source parameters that govern PDC initiation and transport (such as volume, velocity, density, temperature and grain-size distribution) are plagued by high uncertainties.

Third, although analogue experiments provide insights into the complex processes that govern granular-fluid and turbulent flow^{33–35}, as well as the multiscale and multiphase processes within density currents, they cannot capture the full complexity of natural PDCs. The material properties and the spectrum of gas–particle interactions inside natural PDCs cannot be completely downscaled to the typical scale of laboratory experiments (that is, several metres)^{36–38}, which limits the ability of experimental approaches to inform theoretical and computational flow models.

To overcome the challenges associated with PDC research, and to advance understanding of the enigmatic inner working of PDCs, volcanologists have traditionally applied a combination of field-based observational and sedimentological techniques^{32,39}, analogue

experiments⁴⁰⁻⁴², and theoretical and computational modelling⁴³⁻⁴⁵. Over time, the approach to understanding PDCs has diversified (see the Supplementary Information) and research has been stimulated by major PDC-forming eruptions, such as Mount St. Helens in 1980 (REFS⁴⁶⁻⁴⁸), Pinatubo in 1991 (REF.⁴⁹), Soufrière Hills in 1995–1999 (REFS^{50–52}) and Merapi in 2006 and 2010 (REFS^{7,53,54}); fundamental and technological advances in computational fluid mechanics55; community-based efforts to synthesize analogue PDCs in large-scale experiments^{35,56,57}; and the increased instrumentation of high-risk volcanoes with geophysical sensors⁵⁸⁻⁶⁰. To address uncertainty, community-wide efforts have now started to develop global databases of PDC source conditions (FlowDat⁶¹, DomeHaz⁶² and GLADIS⁶³), which capture frequency versus magnitude relationships of PDC occurrence, mass partitioning during column-collapse-derived PDCs and the volumes of PDCs formed by lava-dome collapse. Nevertheless, examining sedimentary records of past eruptions remains the dominant method in PDC research and continues to guide, apply and test model developments.

In this Review, we discuss recent advances in field-based, theoretical, experimental and numerical studies, which provide insights into the critical complexity of PDC internal flow dynamics. We then consider how geophysical monitoring of natural PDCs can provide insight into their internal flow structure and, thus, constrain experimental and numerical models of PDC dynamics. Finally, through identifying areas of continued uncertainty, we outline future research directions that are required to develop robust hazard models that can reliably assist risk mitigation.

Probing PDC deposits

Recent PDC-forming eruptions provide volcanologists with opportunities to reconstruct the chronology of events8,10 and to obtain high-resolution data of hazard footprints^{20,64}, flow paths^{17,65} and the distribution of dynamic pressure^{20,66} and temperature⁶⁷⁻⁶⁹ before fragile deposits are degraded or removed. In some cases, observations of recent PDCs have enabled estimates of local bulk and frontal velocities 7,53,70, time-integrated bulk-flow densities^{20,66,70} and flow temperatures⁶⁷ to be made, allowing broad characterization of PDC behaviour. Data sets from recent eruptions are critical for defining the input and boundary conditions of computational PDC flow models. Furthermore, they provide real-world scenarios for model validation, calibration and advancement. However, to quantitatively understand the internal flow dynamics within PDCs, and the generation of associated hazards, we need to characterize the evolution and vertical distribution of the velocity, density and temperature within PDCs.

Qualitatively, properties such as the velocity, density and temperature of PDCs are, at least partially, preserved in their deposits. Indeed, lithofacies characterizations of PDC deposits propounded the original interpretation that there are two main types of PDCs^{71–73} (FIGS 1a,2): fully dilute, fully turbulent PDCs with thin tractional bedload regions (pyroclastic surges)^{66,74–77}, and granular-fluid-based PDCs, comprising

Dynamic pressure

One-half of the product of flow density and the squared flow velocity. A measure of the destructiveness of pyroclastic density currents.

Compressible turbulent flow

Turbulent flow where the density and temperature change with gas pressure.

Pore-pressure-modified granular flow

Granular flow where excess pore pressure is present and can alter the friction force inside the flow

Dry granular flow

A dense flow of dry granular material whose dynamics are envisaged to be dominated by the stresses associated with particle–particle interactions, rather than hydrodynamic stresses.

Pyroclastic flows

Pyroclastic density currents dominated by concentrated transport.

Pyroclastic surges

Pyroclastic density currents dominated by dilute transport.

gas pore-pressure-modified granular flow in a lower underflow region and dilute turbulent transport above (pyroclastic flows)^{65,78–80}.

Over the past 50 years, however, conceptual models of the internal structure of PDCs have evolved, guided by advances in the fields of gas fluidization, granular flow, aqueous gravity currents and disperse multiphase flows^{1,32,81–83}. Although early concepts envisaged a longitudinally evolving flow structure dominated by distinct (dilute or concentrated) transport behaviours^{13,71,84}, physical modelling and interpretation of PDC deposits point to a strong vertical density stratification in all PDCs^{85,86}.

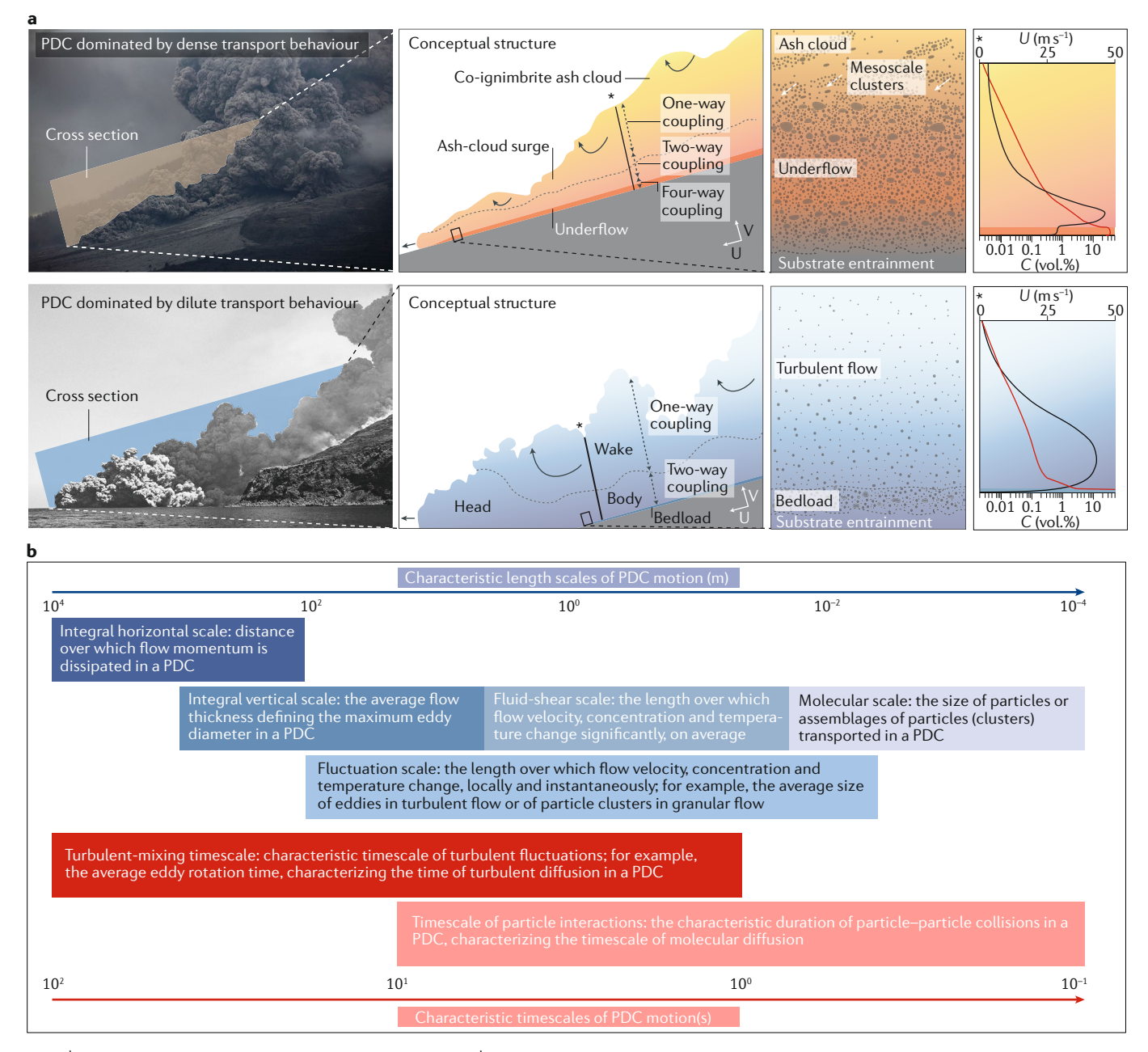


Fig. 1 | Conceptual models and multiscale spectra of PDCs. a | Pyroclastic density current (PDC) from Sinabung volcano in 2014, as an example of a PDC that is dominated by concentrated gas-particle transport (top), and a pyroclastic surge from Stromboli volcano in 2019, exemplifying PDCs with dominantly dilute gas-particle transport (bottom). The left-hand panels display images of the two PDCs, with coloured areas outlining transects that are used to show the conceptual structure of dilute and concentrated PDCs (middle-left panels). The conceptual models of the internal flow structure of concentrated and dilute PDCs reveal their respective height-variant-dominant gas-particle-coupling mechanisms and PDC flow regions. Close-ups of the lower regions of the PDCs (middle-right panels) highlight the presence of gas pore-pressure-modified granular-fluid-based

underflow in concentrated PDCs and a bedload region in dilute PDCs. The right-hand panels display generalized vertical profiles of time-averaged velocity (*U*) and volumetric particle concentration (*C*) for dominantly concentrated and dilute PDCs (the locations of the velocity profiles are marked by the vertical lines in the middle-left panels). **b** | The characteristic length scales (blue bars) and timescales (red bars) that govern PDC transport behaviour and their fluid-mechanical meaning (based on REFS^{199,200}). The wide, and partially overlapping, length scales and timescales of PDC transport behaviour result in a broad spectrum of concurrently occurring gas—particle, particle—particle and particle—eddy feedback mechanisms inside PDCs. Part **a** images courtesy of Photovolcanica (top) and Alberto Lunardi (bottom).

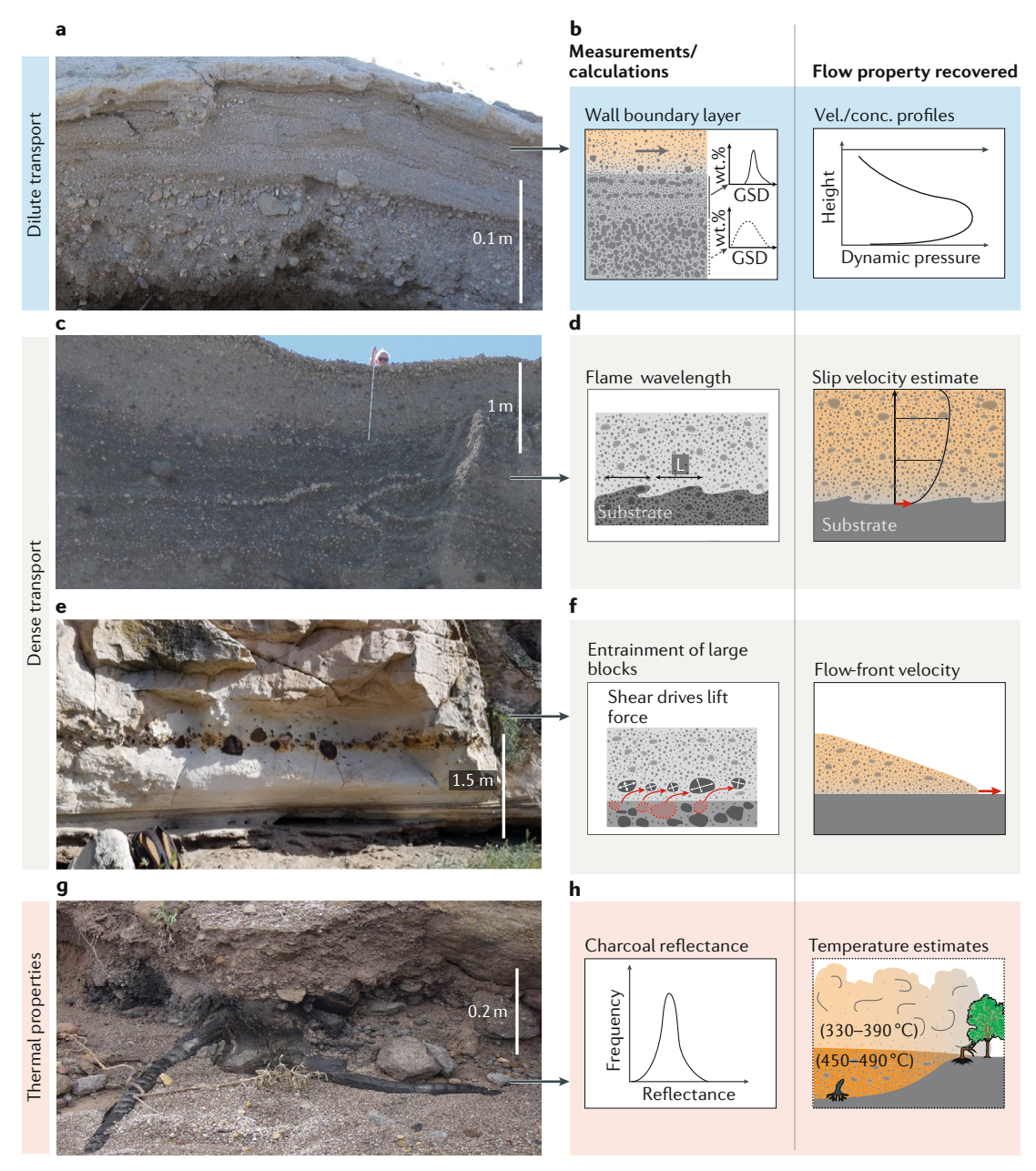


Fig. 2 | Approaches to estimate flow velocity, density and temperature from deposit characteristics. a | Tripartite and upward-fining deposit of dilute pyroclastic density current (PDC) transport from the 2012 hydrothermal blast of Te Maari (New Zealand). b | The grain-size distribution (GSD) of stratified PDC deposits can be inverted to estimate time-averaged velocity, density and, therefore, dynamic pressure profiles using turbulent-boundary-layer theory 87 . c | Flame structures in the 1980 pumice flow deposit of Mount St. Helens (concentrated PDC deposit). Flame structures are interpreted as 'frozen' shear instabilities. d | Analyses of the wavelength of flame structures allows the local slip velocity and sedimentation rate of concentrated PDC transport to be estimated 97 . e | Entrained blocks in the lower metre of the Peach Spring Tuff: large blocks can be entrained by concentrated PDCs, owing to a lift force generated during flow slips across the substrate 95,100 . f | Clast trains can be used to calculate the flow-front velocity of concentrated PDCs. g | Charred wood at the base of a block-and-ash flow deposit from Soufrière Hills. h | Charcoal reflectance 54,201 is commonly used to estimate the local flow temperatures at the base and in the lower few metres of PDCs.

Whether the density stratification is associated with abrupt changes or with a gradual continuum in particle concentration remains uncertain³⁴. As a result, several strategies have been adopted to quantitatively determine the transport parameters of PDCs from their deposits, building upon the original simple distinction between dilute and concentrated PDCs.

For dilute currents, turbulent-boundary-layer theory and sediment-transport hydraulics can be used to infer flow properties from deposit characteristics. For example, particle size, shape and density information of stratified PDC deposits (FIG. 2a) is regularly used to reconstruct profiles of the local time-averaged velocity and density flow structure^{87–89} (FIG. 2b). As a result, volcanologists

Polydispersity

The characteristics of a mixture of particles that contains a range of particle sizes.

Isotropic turbulence

An idealistic state of turbulence, where turbulent fluctuations are assumed to decay statistically uniformly in every direction.

Pore pressure

The pressure of the fluid contained in the interstices of a granular medium.

can capitalize on the deposits of dilute PDCs to estimate vertical profiles of destruction-causing dynamic pressure, which is essential for future hazard assessments. However, it remains unclear how gas-particle turbulence, heat, polydispersity and wall shear on natural rough surfaces modify energy dissipation, stratification and particle sedimentation inside dilute PDCs.

In addition, the median diameter of stratified PDC deposits can be related to the eddy rotation speed ΔU (REFS^{90,91}), and to a local mean flow velocity⁹², by approximating the conditions of gas–particle decoupling and turbulent sedimentation from large eddies. Analysis of PDC deposits can, therefore, reconstruct spatial variations in flow velocity from past PDC-forming eruptions. However, there are critical assumptions behind the calculation of mean flow velocity from analysis of stratified PDC deposits, such as the decaying isotropic turbulence spectrum, which require future validation.

Dilute PDCs, in their most hazardous flow-outrun regions, tend to be temporally non-depositional and erosive, which limits the use of the above two methods for hazard assessments. In such cases, however, the local bulk-flow density of dilute PDCs can be estimated through modelling the reattachment distance of temporally airborne PDCs⁹³. Iterative modelling of PDC reattachment has recently been applied to the 1980 blast of Mount St. Helens, confirming independent density estimates.

For concentrated PDCs, identifying relationships between the deposit characteristics and the dynamics of gas–particle transport remains challenging. Recently, an empirically and experimentally derived model linked the formation of granular shear instabilities, such as flame structures, to internal slip velocities such as flame structures, to internal slip velocities such as flame structures, to internal slip velocities such as flame velocities has been used to provide local estimates of sedimentation rates during aggradation of the 1980 Mount St. Helens pyroclastic flow (FIG. 2c,d). Sedimentation rates of 4–32 cm s⁻¹, in combination with estimates of flow duration, demonstrate that PDC deposition is characterized by minute-long periods of non-depositional PDC bypass alternating with seconds-long intervals of strong deposition.

Additionally, experiments have related the dynamic lifting of particles, owing to gradients in gas pore pressure inside flows, to frontal velocity 98,99 (FIG. 2e,f). Analysis of dynamic particle uplift has since been used to estimate the flow-front velocity of enigmatic long-runout PDCs generated in explosive volcanic super-eruptions (5–20 ms $^{-1}$ for PDCs forming the 18.8-Ma Peach Spring Tuff), which were never directly witnessed 100 (FIG. 2e,f). Furthermore, application to the May 18 1980 PDC of Mount St. Helens suggests surprisingly low fontal velocities of c. 10–13 m s $^{-1}$ at c. 5–6 km from the vent 98 , in agreement with observed flow-front velocities (7–10 m s $^{-1}$) at the same distance during the 7 August 1980 eruption 101 .

The high temperature of PDCs (around 60 °C for the coldest PDCs and up to magmatic temperatures for the hottest PDCs), and, hence, the buoyancy of the interstitial fluid, sets them apart from other natural-gravity currents¹⁰². However, the influence of temperature on

the dynamics of PDCs remains poorly constrained. New advances in thermal proxies, including palaeomagnetic and charcoal-reflectance techniques (FIG. 2g,h), allow volcanologists to map temperature variations across PDC footprints^{69,103,104} and provide new avenues to characterize PDC stratification conditions⁶⁸.

Despite the large number of insights provided by studying PDC deposits, it is important to consider some shortcomings of the methods described above. For example, deposit-based estimates of PDC velocity, density and temperature cannot capture temporal changes in the bypassing PDC, which may be critical to the evolution of PDCs and the intensity of hazard impacts⁵⁶. Furthermore, internal feedbacks between polydispersity, temperature and pore pressure are expected to occur, but are not currently captured in empirical models of concentrated PDC transport.

Indeed, recognition of the effects of fluid drag in the interplay of polydisperse particle settling, gas pore-pressure generation and upward gas migration has added new momentum to the debate surrounding the origin of tens-of-metres-thick sheets of massive PDC deposits extending tens to hundreds of kilometres from their source. Several distinct hypotheses on the underlying flow-transport mechanism of PDCs¹⁰⁵⁻¹⁰⁸, invoking both dilute and concentrated transport regimes, have been proposed to explain these massive PDC deposits. However, analysis of the effects of fluid drag on the evolving density stratification within PDCs, which cannot be captured in their depositional records, helps to discriminate between deposits formed by dilute and concentrated flow.

An empirical PDC-transport parameter $T_{\rm de-di}$ discriminates between deposits of dominantly dilute PDCs, which are unable to generate an underflow with elevated gas pore pressure, and concentrated transport regimes, which can generate mobile underflows. The non-dimensional ratio quantifies the flow mobility from a PDC deposit by assessing its runout length, inundation area and the role of the hydraulic permeability, which controls the gas pore pressure and, thus, friction on the PDC in the lower flow boundary:

$$T_{de-di} = \frac{A^3 d_{s,1/2}}{V^{5/3} I^2} \tag{1}$$

where A and V are the deposit footprint area and volume, respectively, and $d_{\rm s,1/2}$ is the effective aerodynamic particle diameter at half of the PDC runout distance L (REF. ¹⁰⁹). Deposits resulting from dominantly dilute PDC transport are characterized by $T_{\rm de-di} > 5 \times 10^{-3}$, while deposits emplaced by dominantly concentrated PDCs have $T_{\rm de-di} < 2.5 \times 10^{-3}$.

The enigmatic internal flow structure

In the last decade, volcanologists have pushed the development of large-scale experiments^{33,35,110} and 3D multiphase flow models^{111,112} to circumvent the limitations associated with PDC deposit interpretations. Numerical multiphase models can generate real-scale flows that interact with topography and capture a large range of

Subgrid models

The representation of physical processes occurring at scales that are not resolved on a computational mesh.

gas-particle coupling regimes encompassing the concentrated to dilute spectrum¹. The models demonstrate the temporal and spatial evolution of the internal structure of PDCs, but are limited in spatial resolution by the large computational cost associated with high-resolution simulations. Subgrid models are required to capture microscale and mesoscale processes (turbulent dissipation, aggradation, particle breakage), but inadequate constraints exist on such processes for volcanic mixtures.

Large-scale experiments can bridge the scaling issues encountered with benchtop experiments and the low resolution of numerical multiphase models. Direct measurements of large-scale experiments provide

insights into the vertical stratification of PDCs^{113,114}. In addition, they can be used to focus on specific concentration regimes (diluta^{35,114} or concentrated regimes of PDCs¹¹⁵) and study evolving flow behaviours as currents develop particle-concentration gradients¹¹⁰ (FIG. 3a).

Delineating dilute, intermediate and concentrated regimes. There is extensive evidence that a single PDC spans a range of concentrations, which can result in abrupt changes in flow behaviour^{32,116}. The particle volume fraction (Φ_V) threshold between dilute and concentrated suspensions is often placed at $\Phi_V \sim 10^{-3}$, delineating two-way from four-way coupling (FIG. 3b,c).

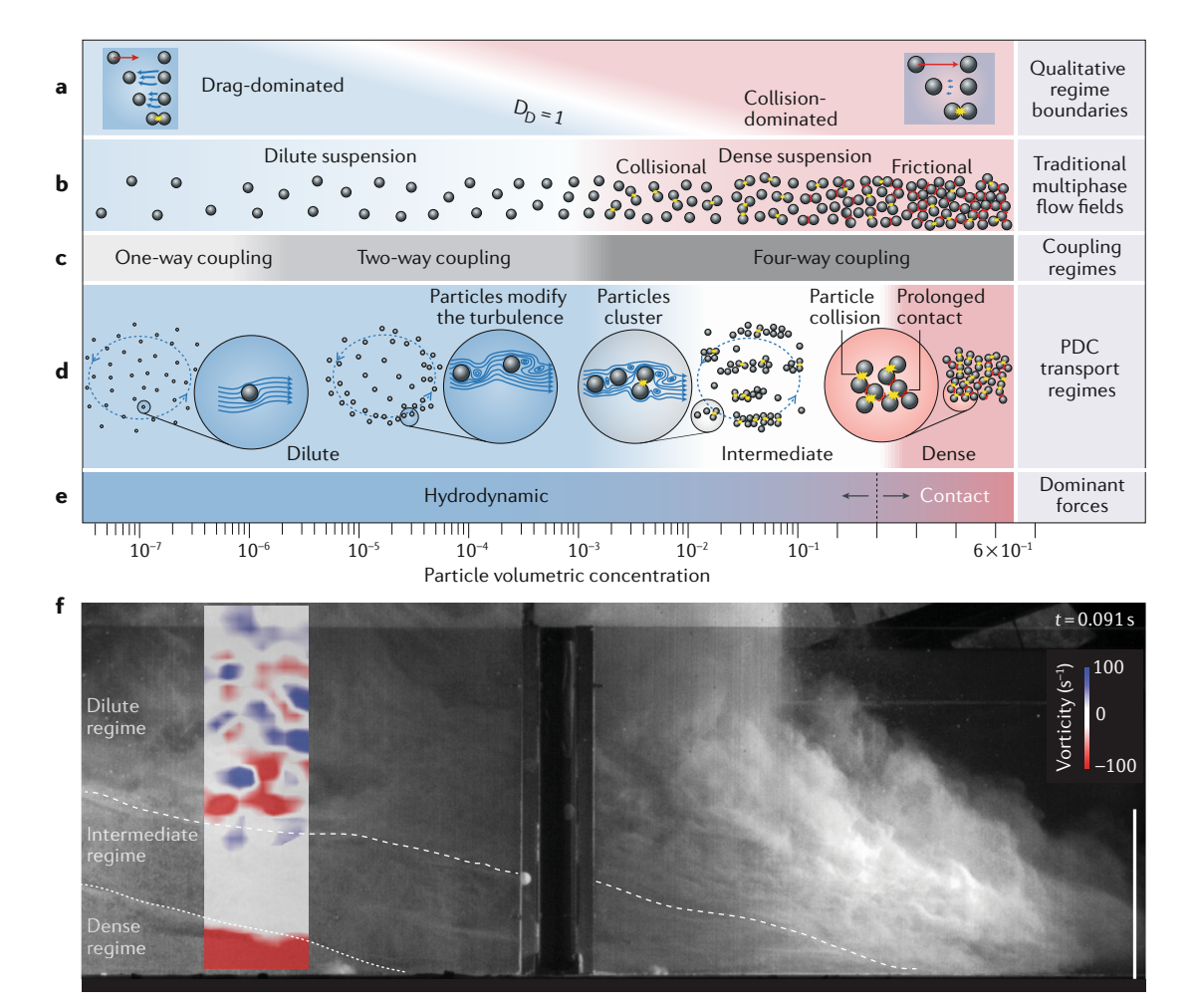


Fig. 3 | **Delineating concentrated, intermediate and dilute transport regimes in PDCs. a** | Discriminating dragdominated and collision-dominated transport regimes through the timescale ratio $D_{\rm D}$ defined by REFS^{91,119}. Existing models of the particle–particle collision timescales cannot yet delineate dilute and concentrated transport regimes quantitatively. **b,c** | A schematic representation of the traditional multiphase flow fields of dilute and dense suspensions (part **b**) and their associated gas–particle-coupling regimes (part **c**) relative to the flows' particle volume concentration. **d** | A schematic illustration, and approximate range in particle concentration, of the dilute, intermediate and concentrated transport regimes of pyroclastic density currents (PDCs). Details of gas–particle feedback mechanisms in each regime are highlighted. Blue arrows represent fluid streamlines, blue dashed lines highlight large eddies. Yellow stars highlight particle collisions and their relative frequency. **e** | The threshold concentration ($\Phi_{\nu d}$) at the intermediate-concentrated boundary, where frictional contact stresses equal hydrodynamic stresses. **f** | Formation of concurrent concentrated, intermediate and dilute transport regimes in large-scale PDC experiments. A contour plot of the vorticity highlights the strong changes in the degree of turbulence. Large variations in the vorticity of the dilute region are associated with large coherent turbulence structures and negative values in the concentrated region are associated with strong downslope-directed shear. A broad range of moderate vorticity values are present in the intermediate regime, highlighting intermediate turbulence intensity. The white line scale in the bottom-right corner is 0.3 m long. Panel **f** is adapted with permission from REE. Elsevier.

Monodisperse

A mixture of particles with equivalent size.

Mesoscale particle clusters Gatherings of particles into coherent band-like structures. In two-way coupling, the motion of particles is affected by the flow of gas around them, and the gas flow, in turn, is affected by the presence of particles¹¹⁷. In four-way coupling, two-way coupling is further modified by particlegas-particle interactions (gas that is compressed between particles, generating lubrication forces)¹¹⁸ and particleparticle interactions (including collisional and prolonged frictional particle-particle contacts)¹¹⁷.

In dilute and concentrated suspensions, momentum exchange can be described by the ratio between the collisional and particle drag response timescales, $D_{\rm D}$ (REFS^{91,119}):

$$D_D = \frac{\tau_c}{\tau_p} \tag{2}$$

where $\tau_{\rm c}$ is the characteristic timescale between particle collisions and $\tau_{\rm p}$ is the characteristic timescale required for gas–particle dynamic forces to influence the flow behaviour of particles inside the flow. For $D_{\rm D}$ <1, particle collisions are too frequent for particles to respond to the gas–particle dynamic forces, while for $D_{\rm D}$ >1, gas–particle forces are dominant (FIG. 3a). However, the mechanisms that influence the two timescales, such as local turbulent fluctuations, changes in gas velocity and particle–substrate interaction, are poorly constrained. Thus, Eq. 2 cannot be used to define an exact concentration threshold between concentrated and dilute regimes.

A drastic change in particle-settling behaviour occurs at a particle volume fraction of $\Phi_{\rm V} \sim 10^{-2}$ (for monodisperse systems), associated with the onset of mesoscale particle-cluster formation¹²⁰⁻¹²². At particle concentrations above this threshold, heterogeneous drag dominates particle-settling velocities and interparticle collisions are frequent. Thus, a particle volume fraction of $\Phi_{\rm V} \sim 10^{-2}$ defines the boundary between the dilute and newly identified intermediate regime (defined by the formation of mesoscale particle clusters) in monodisperse systems¹²¹ (FIG. 3d). In large-scale PDC experiments using natural polydisperse volcanic mixtures, clustering occurs at $\Phi_{V} = 1 \times 10^{-2.6}$ (G.L., E.C.P.B., T.E.-O. and J.D., unpublished observations), close to the traditional boundary between dilute and dense suspensions¹¹⁹. Therefore, the concentration boundary between the dilute and intermediate regimes in PDCs might range from 10⁻² to 10⁻³, although the role of polydispersity on the onset of mesoscale clustering needs further quantification.

In engineering studies of monodisperse suspensions and large-scale PDC experiments containing polydisperse particles, clustering vanishes at $\Phi_{\rm V}>3-4\times10^{-1}$. At greater particle concentrations, the gas–particle dynamics become dominated by prolonged frictional particle contacts 34,121,123 , defining the concentrated regime. The observed intermediate-concentrated boundary ($\Phi_{\rm V}\sim3-4\times10^{-1}$) can be quantified by the condition where the contact (that is, frictional) contributions overcome the hydrodynamic contributions to the granular shear stress. Therefore, by equating frictional and hydrodynamic stress, the intermediate-concentrated boundary can be located at a critical solid fraction of $\Phi_{\rm V}=\Phi_{iid}\sim3\times10^{-1}$, consistent with experimental findings (FIG. 3e). However, to assess the variability of the

intermediate-concentrated boundary for PDCs with different grain-size distributions, we need to derive the material constants and friction laws for pyroclastic mixtures. Concurrent dilute, intermediate and concentrated flow regimes have recently been observed in large-scale PDC experiments³⁴, which demonstrate that all three regimes are present in a wide range of flows and, therefore, the properties of all regimes must be considered (FIG. 3f).

The concentrated regime. The dynamics of gas-particle transport and deposition in concentrated PDCs $(\Phi_V \gtrsim 3 \times 10^{-1})$ have traditionally been investigated through analogue experiments on high-density turbidity currents38,124, dry granular flows125-127 and gas-fluidized granular flows^{40,127,128}. Alongside principles of aqueous and aeolian sediment transport, such studies guide current interpretations of PDC deposits32,39,129. However, the insights gained from the analogue experiments and the application of aqueous and aeolian sediment-transport analogies are limited by conditions that are unique to PDCs, including: high fluid-to-particle density contrasts; large particle-size distributions; and low viscosities of the fluid phase. Conditions specific to PDCs can be demarcated from those of other mass flows through three non-dimensional numbers: the granular Stokes number St_{eranular} , the particle Reynolds number Re_n and the drag-normalized particle-to-fluid density ratio r (REF. 130):

$$St_{granular} = \frac{\alpha d_p \sqrt{\rho_s P_s}}{\eta_f} \sqrt{\frac{2}{3}}$$
 (3)

$$Re_{p} = \frac{\alpha d_{p} \sqrt{\frac{2}{3} P_{s} \rho_{f} C_{d}}}{\eta_{f}} \tag{4}$$

$$r = \sqrt{\frac{\rho_s}{\rho_f C_d}} = \frac{St_{granular}}{Re_p} \tag{5}$$

where $\rho_{\rm f}$ and $\eta_{\rm f}$ are the fluid density and dynamic viscosity, respectively; $\rho_{\rm s}$ is the solid density; $C_{\rm d}$ is the drag coefficient; $P_{\rm s}$ is the normal stress; $d_{\rm p}$ is the product of the effective aerodynamic particle diameter (Sauter mean diameter) and the average particle sphericity, chosen to account for the mean hydrodynamic drag of a collection of polydisperse particles 131,132 ; and α is related to the permeability k of the mixture as follows 133 :

$$\alpha = \frac{k}{d_p^2} \tag{6}$$

The conditions $St_{\rm granular} = 1$, r = 1 and $Re_p = 1$ delineate three regimes where particle settling is dominated by viscous drag, inertial drag or gravity¹³⁰ (FIG. 4a). Natural PDCs fall exclusively into the gravitational regime, owing to their unique particle-to-gas density ratio, high fine-ash content and low viscosity of the

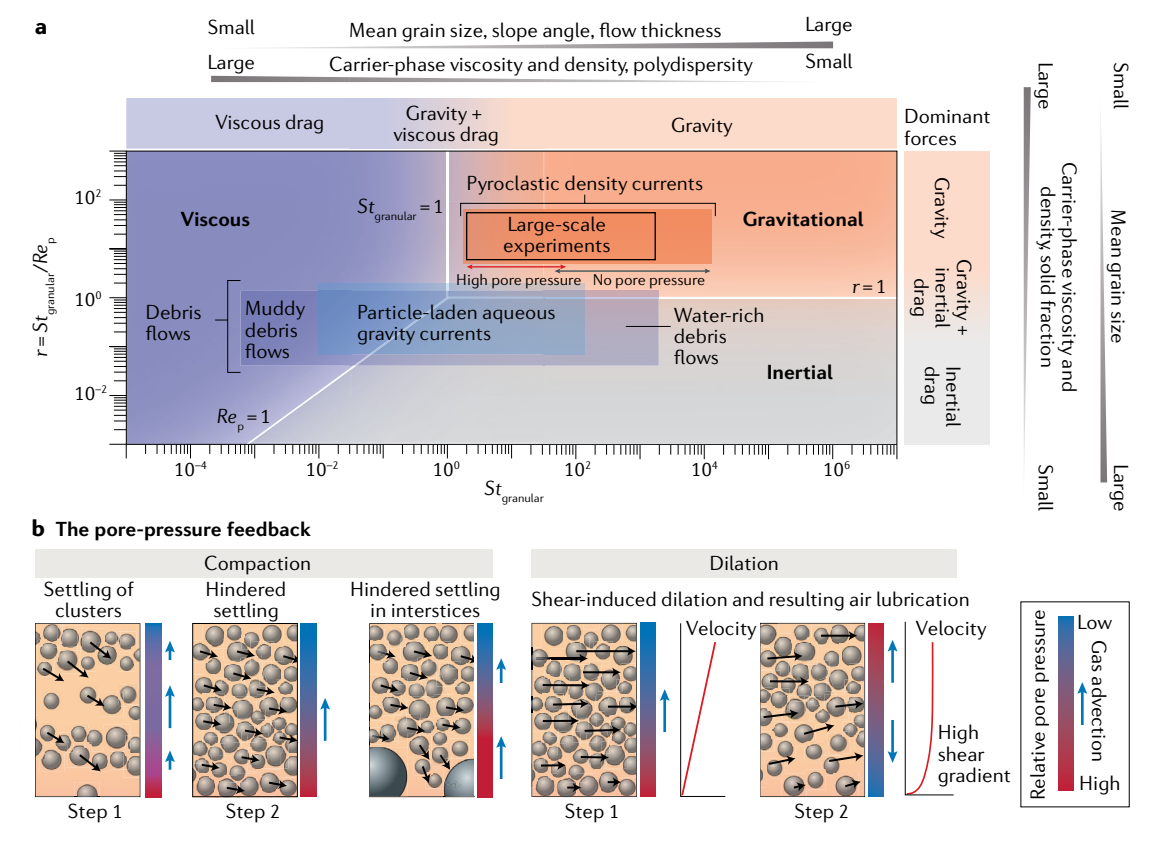


Fig. 4 | Concentrated transport regimes of PDCs. a | Different behaviours of dense granular-fluid flows can be delineated using the granular Stokes number ($St_{granular}$), the drag-normalized particle-to-fluid density ratio (r) and the particle Reynolds number (Re_p). The fields where viscous drag, inertial drag and gravitational forces dominate are highlighted (based on REF. ¹³⁰). Natural pyroclastic density currents (PDCs; with and without elevated pore pressures), and large-scale PDC experiments using natural volcanic particles and air, fall into the gravitational field. Debris flows and high-density particle-laden aqueous gravity currents occupy the viscous drag-dominated and inertial-drag-dominated fields. **b** | The spectrum of known pore-pressure feedback mechanisms through flow compaction, dilation and shear conditions. The colour bar represents the relative pore pressure in the domain and the blue arrows display the direction for gas advection. Black arrows depict the velocity vector for the solid phase. Schematic velocity profiles for shear-induced dilation and resulting air lubrication reveal that shear gradients disrupt unidirectional and upward-directed gas advection and force strong downwards gas advection into a thin gaseous boundary layer.

dusty gas phase. Large-scale PDC experiments¹¹⁰ cover a large proportion of the PDC field and, similarly to gas-fluidized granular-flow experiments, are well scaled to PDCs. Conversely, experiments using aqueous fluid phases fall within the viscous drag-dominated and inertial-drag-dominated regimes that characterize natural debris flows and turbidity currents (FIG. 4a). Thus, water–particle analogues should not be used to study concentrated PDC transport behaviour.

The concentrated regime of PDCs is characterized by a wide range in the granular Stokes number (10^{o} – 10^{4} ; FIG. 4a), which can be related to a spectrum of flow behaviours spanning dry granular flow (high $St_{\rm granular}$) to porepressure-modified granular flow (low $St_{\rm granular}$). In dry granular flow, fluid hydrodynamic drag is low and gravity, friction and contact forces dominate. In pore-pressure-modified flow, gravitational forces remain dominant. However, the gas phase modifies particle motion through drag and lift forces, which can partially or fully balance the effect of gravity and, in association with elevated gas pore pressure, reduce the interparticle friction 134 .

Although gas pore pressure cannot yet be measured in natural currents, evidence from field studies 101,108,135 , numerical simulations 109,111,136 and experiments 131,137,138 indicate that the low permeability of PDCs enables self-generation and retention of pore pressure for long durations (minutes to hours) 131,139 . Specifically, elevated gas pressures can be retained in the concentrated regime of PDCs, as their high polydispersity and abundance of fine ash endows them with a low effective aerodynamic particle size and, subsequently, a low permeability (down to 10^{-12} – $10^{-13}\,\mathrm{m}^2$) 131,139 .

A variety of feedback mechanisms between the solid fraction and pore pressure in PDCs¹⁴⁰ are key to the formation and modulation of pore pressure, and occur during local flow compaction and dilation. During compaction, elevated pore pressure can be self-generated by several mechanisms, including: rapid particle settling from intermediate concentrations ($10^{-2} < \Phi_{\rm V} < 3 \times 10^{-1}$) by column collapse^{141,142}; rapid settling of mesoscale clusters¹²¹; hindered settling, where particles fall into interstices in the substrate^{143,144}; or through local changes in solid fraction within a dense bed¹⁴⁰ (FIG. 4b).

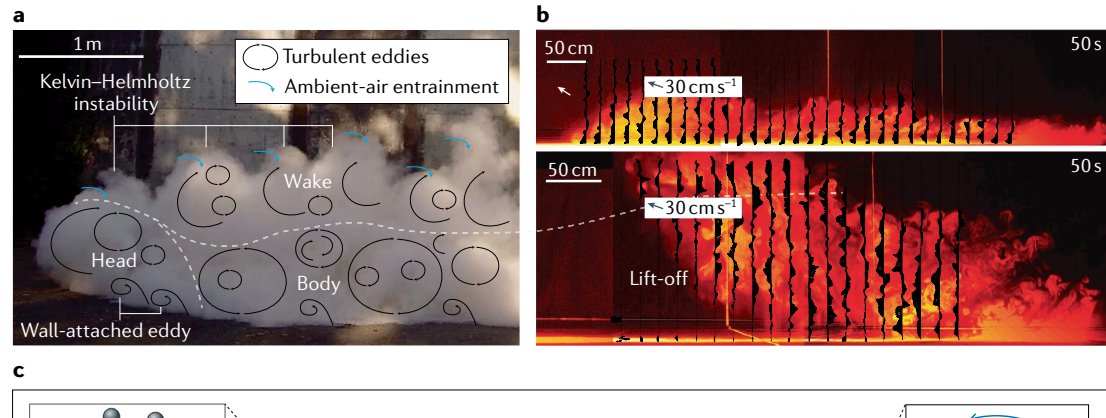
Kolmogorov scale

The length, time and velocity scales in turbulent flows below which the effects of molecular viscosity are non-negligible.

Conversely, local dilution associated with the formation of strong vertical shear gradients at the base of a PDC leads to gas moving towards this 'low'-pressure region¹³⁴ and subsequent air lubrication of the basal portion of the flow (FIG. 4b). The gas flow and drag associated with pore-pressure advection alleviate the high frictional properties of volcanic material, which limits the influence of basal friction^{109,134} and enables the dense mixture to propagate for long distances of tens of kilometres and on shallow slopes.

The relative effectiveness and interdependence of the different pore-pressure feedback mechanisms in real-world flows remain to be shown. A major challenge for future studies lies in the development of a granular-fluid rheology that can capture the effects of transient pore-pressure feedbacks (and implementation into large-scale flow models). However, the rheology of hot and polydisperse volcanic mixtures in the concentrated regime is still poorly understood ¹⁴⁵. Furthermore, complex transient processes, such as particle breakage ⁴⁴, attrition ¹³⁷ and segregation ¹⁴⁶, propagation over rough substrate ^{97,100} and changes in shear-rate gradients ¹³⁴ owing to slope variations, are still unaccounted for in the concentrated regime.

The dilute regime. The upper flow region of dense PDCs and the major proportion of dilute PDCs are traditionally considered to behave as a fully dilute and fully turbulent suspension. The dynamics of the dilute turbulent regime ($\Phi_{\rm V} < 10^{-3}$ to 10^{-2}) is dominated by eddies with diameters comparable to the flow height (excluding the wake) down to the Kolmogorov scale⁸⁵ (FIG. 5a). In this regime, particle–particle interactions are rare and particle transport is dominated by fluid drag and gravity. Eddies modify PDC dynamics in several ways, including: dissipation of energy from large to smaller scales⁹²; delaying particle



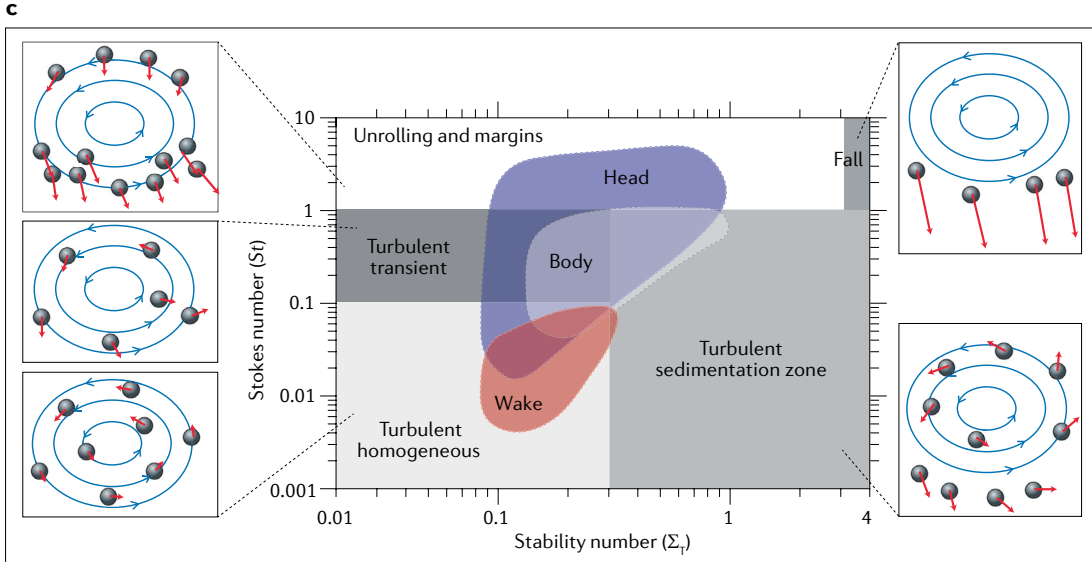


Fig. 5 | The dilute turbulent transport regime. a | Structure of an experimental pyroclastic surge. Turbulent eddies and Kelvin–Helmholtz instabilities promote entrainment of ambient air. b | Comparison of the velocity structures in ambient-temperature (top) and heated (bottom) dilute pyroclastic density current analogues. While the gravity current structure in the cold flow is well defined, complex velocity fields, buoyancy reversal and lift-off occurs in the hot flow. c | Particle-transport regimes in turbulent eddies. Data taken from a large-scale dilute pyroclastic density current experiment shows the wide range of particle-transport regimes of particles in turbulent eddies, as described in REFS^{91,119}, are illustrated as sketches. In turbulent homogeneous transport, particles follow gas streamlines. In transient and turbulent sedimentation regimes, particles detach from streamlines and their settling is delayed by the rotating motions of eddies. In the unrolling and margins regime, particles segregate towards eddy peripheries and mesoscale clusters form. In the fall regime, particles are negligibly affected by the eddies. Part b adapted from REF. Springer Nature Limited. Part c adapted with permission from REF. Elsevier.

Kelvin-Helmholtz instabilities

A hydrodynamic instability in which immiscible, incompressible and inviscid fluids are in relative and irrotational motion.

Lift-off distances

The distance at which the flow density becomes lower than that of ambient air, resulting in the buoyant rise of part of the pyroclastic density current.

settling by actively mixing the flow¹⁴⁷; and contributing to ambient-air entrainment^{114,148} (FIG. 5a,b).

PDCs composed of rock and hot gas can only propagate as a gravity current as long as the mixture density exceeds that of the ambient atmosphere¹⁴⁹. The density of PDCs can be modulated through simultaneous entrainment of material from the substrate (which increases its density)¹⁵⁰ and, importantly, dilution and a decrease in density through particle settling and entrainment of ambient air. The resulting changes in density strongly influence the flow velocity.

Turbulence enhances entrainment of ambient air through Kelvin-Helmholtz instabilities at the free surface^{114,151,152} (FIG. 5b). Entrainment is largely controlled by the flow stratification 111,152 and modifies the thermal stratification and density of the current. Large-scale experiments have shown that the extent of air entrainment can be parameterized by a value known as the entrainment coefficient, which typically varies between 0.1 and 0.2 and can locally reach values of 0.4-0.5 in the head of the current^{56,114,153}. The entrainment coefficient is locally variable within a certain flow and values >0.2 are associated with vigorous entrainment of ambient air. Because turbulent entrainment reduces the density contrast between the current and the ambient air, reducing its final runout and lift-off distances, parameterizations of the entrainment coefficient are important in models where air entrainment is not captured by the governing equations.

In addition, settling of particles from turbulent eddies, which further dilutes the current and modifies its density stratification, is critical for the evolution of PDCs in the dilute regime. The Stokes number describes the ratio of a characteristic particle response time (such as the settling timescale) to a characteristic fluid timescale (such as the eddy overturn time):

$$St = \frac{1}{f} \frac{\Delta \rho d^2 \Delta U}{18\mu_o \delta} \tag{7}$$

where ΔU is the eddy rotation speed, d is the particle diameter, δ is the eddy diameter, $\mu_{\rm g}$ is the dynamic viscosity of the gas and $\Delta \rho$ is the difference in density between the solid and the gas. f is a drag factor related to the particle Reynolds number. For $St \ll 1$, particles couple with the gas and closely follow fluid streamlines, for $St \sim 1$, particles segregate towards eddy peripheries and for $St \gg 1$, particles decouple from the turbulent mixture. Another important parameter is the stability number $(\Sigma_{\rm T})$, which assesses the gravitational force acting on particles within dilute PDCs and evaluates whether particles will separate from eddies.

$$\Sigma_T = \frac{U_T}{\Lambda U} \tag{8}$$

where U_T is the settling velocity of particles in the fluid. Particles only separate from eddies when $\Sigma_T \gg 1$.

Particle-eddy interaction in the dilute regime can be categorized into five gas-particle transport regimes, based on theoretical modelling and observations from large-scale experiments, namely: unrolling and margins of eddies (St > 1; $\Sigma_T < 3$), turbulent sedimentation (St < 1; $\Sigma_T > 0.3$), turbulent transient (0.1 < St < 1; $\Sigma_T < 0.3$), turbulent homogeneous (St < 0.1; $\Sigma_T < 0.3$) and fall (St > 1; $\Sigma_{\rm T} > 3)^{56,91}$ (FIG. 5c). Large-scale experiments show that multiple gas-particle transport regimes coexist in a single current and dominate in spatially distinct portions of the flow (FIG. 5c). The results from large-scale experiments have important implications for numerical models of dilute PDCs, which traditionally assume that gas and particle phases are nearly homogeneously suspended inside a PDC and have negligible feedbacks. Future research should be focused on understanding the mechanism and associated constitutive relationships that govern gas-particle transport within and out of large eddies, to characterize particle-settling conditions in lower-order PDC flow models.

The intermediate regime. The recently discovered intermediate regime (10^{-3} to $10^{-2} < \Phi_{\rm V} < 0.3$) is characterized by an inhomogeneous distribution of particles, resulting in mesoscale particle clustering 154,155 . Currently, three mechanisms of cluster formation are recognized (FIG. 6a): collision-induced, drag-induced and wake-induced. In collision-induced clustering, particle–particle frictional and inelastic contacts dissipate the granular temperature of the mixture and, therefore, the energy required to homogenize the gas–particle suspension 156,157 .

Alternatively, in the presence of a fluid, viscous drag and mean drag effects can result in drag-induced instabilities and clustering. Viscous drag relates to the increased drag force operating on two particles in the vicinity of each other, which decreases their relative mean velocity prior to collision and increases the probability of clustering. The mean drag effect refers to an instability driven by the volumetric particle concentration control on the slip (the presence of relative velocity) between gas and particles 158. As gas tends to bypass regions with higher particle concentrations, resulting in a decrease of drag on these particles, clusters grow as particles in denser regions fall rapidly and capture particles from slower-settling, more dilute regions.

Finally, wake-induced clustering, where reduction of drag on a trailing particle in the wake of another particle leads to clustering, is especially important in fines-rich polydisperse systems, owing to the stronger relative influence of drag on smaller particles compared with larger particles ^{159,160}. Wake-induced clustering will only occur if the particle Reynolds number in a polydisperse suspension exceeds a critical value of 275.

Regardless of the mechanism, mesoscale clustering changes the properties of volcanic mixtures and can enhance settling in intermediate-concentration regimes^{34,120,155}. In large-scale PDC experiments, dendritic mesoscale clusters, which attain lengths of several decimetres, settle at terminal velocities twofold to threefold that of particles in dispersed suspensions³⁴ (FIG. 6b,c). Mesoscale clustering can, as a result, explain the formation of elevated gas pore pressure inside PDCs¹¹¹ and corresponds to what has been long hypothesized as rapid suspension sedimentation⁵¹. Furthermore, high-resolution multiphase simulations

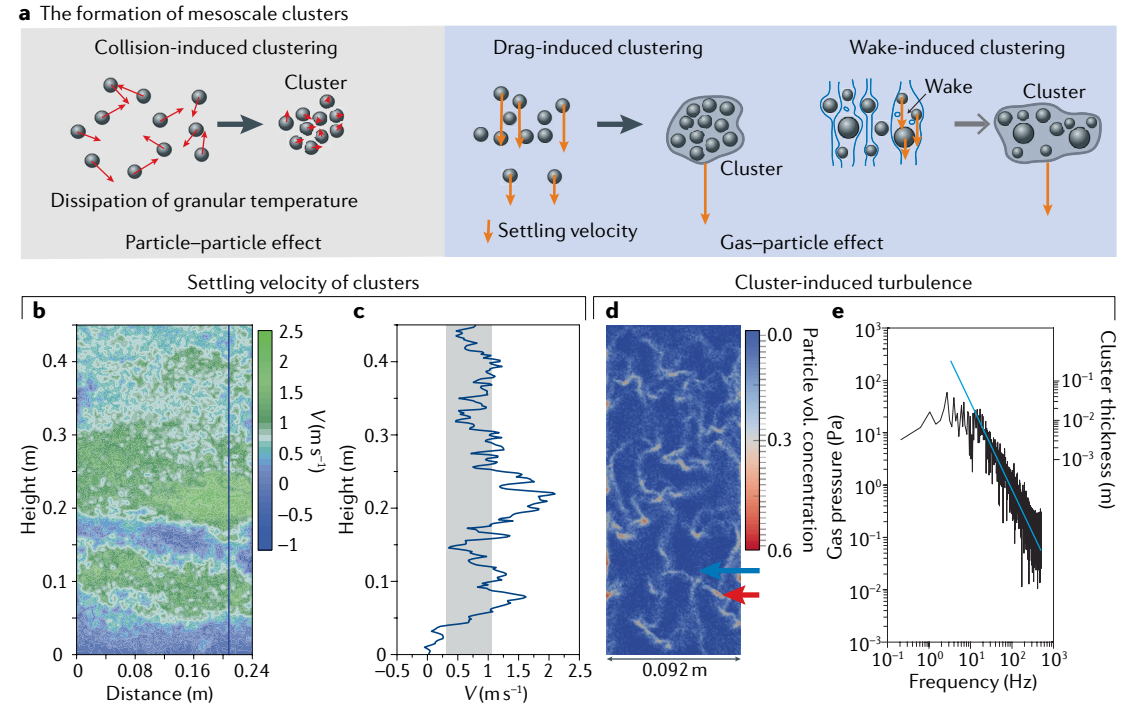


Fig. 6 | The intermediate transport regime. a | The three mechanisms of mesoscale cluster formation. In collision-induced clustering, the granular temperature strongly declines. During drag-induced clustering, particles in denser regions settle faster than particles in dilute regions and incorporate these particles into larger clusters. During wake-induced clustering, drag reduction in the wake of large particles grows fast-settling clusters. b | Contour plot of the vertical velocity component V in the lower 0.45 m of a large-scale dilute pyroclastic density current experiment. Fast-settling mesoscale clusters are associated with high vertical velocities. c | Vertical velocity against flow height for the location marked by the blue line in part b. The vertical grey bar represents the settling velocity of the mean grain-size diameter of the mixture in this flow region. d | High-resolution multiphase simulation of a settling suspension of spherical glass beads in air (mean particle volumetric concentration of 7 vol.%). The suspension segregates into band-like high-concentration domains of mesoscale clusters (red arrow) separated from low-concentration neighbouring regions (blue arrow). Cluster-induced turbulence is generated through the fast settling of mesoscale clusters displacing air upwards. e | The frequency spectrum of local gas pressure for the simulation shown in part d. The typical thickness of mesoscale clusters associated with different gas-pressure values are displayed on the second y-axis. The frequency of clusters (and average cluster thickness) decline with decreasing gas pressure. The decay of the gas pressure with increasing frequency follows a slope of -5/3 (blue line). which is generally observed in homogeneous turbulent fluid flows with a cascade of eddies that dissipate the excess turbulent energy. Part **d** adapted with permission from REF. 109, Wiley.

of settling suspensions show that the formation of clusters self-generate gas turbulence through gas-pressure fluctuations ¹⁶¹ (FIG. 6d). The turbulence energy resulting from a spectrum of millimetre-thick to centimetre-thick clusters is similar to that known to occur for the inertial range of eddies in fully turbulent flows (FIG. 6e). Therefore, simulations of settling suspensions appear to contradict the common assumption that fluid turbulence in gravity currents is hampered in dense suspensions with particle volume fractions exceeding ~1 vol.% (REF. ³²).

The intermediate regime is the least understood of the three concentration regimes presented here. The understudied nature of the intermediate regime is, in part, due to its transient nature, which makes it hard to investigate experimentally. Moreover, in the intermediate regime, gas-particle, particle-gas-particle and particle-particle interactions occur simultaneously, adding intrinsic multiphase complexity. It is, however, a regime that requires attention, as its controls the coupling between the dilute and concentrated regimes, as well as density stratification and particle settling in

PDCs. In addition, mesoscale clustering in the intermediate regime influences the rate of mass loss (through sedimentation) and momentum (through viscosity and friction). Consequently, drag law corrections and subgrid models that account for mesoscale clustering must be developed. Implementation of such subgrid models, within both two-layer depth-averaged models and multiphase models, will help to predict the flow kinematics, the capacity to overcome topographic obstacles and the PDC final runout distance.

Insights from geophysical measurements

Three-dimensional multiphase simulations and laboratory experiments provide new insights into the flow structure of PDCs. However, we still lack comprehensive measurements of real-world flows to test and advance theory-based and experiment-based knowledge of PDCs. Although the energy and destructive impact of PDCs hamper direct observations, remote geophysical measurements provide an opportunity to probe the physics and structure of flows during their propagation.

Geophysical observations of PDCs are sparse, primarily because of the unpredictability of PDCs and the uncertainty and logistical challenges in optimally placing sensors before an eruption. Nevertheless, geophysical data are required to constrain the macroscale and microscale processes operating within PDCs, and, thus, validate and improve existing empirical, analytical and numerical flow models before they can be confidently applied to forecast PDC hazards. Furthermore, direct geophysical measurements of the length scales, timescales and energy scales of hot gas-particle transport inside PDCs will inform fluid-dynamic and thermodynamic scaling relationships, understanding of gas-particle dynamics in the dilute, intermediate and concentrated regimes, and guide the focus of future laboratory and computational PDC experiments.

Satellite measurements represent one endmember of geophysical observations and can provide valuable information during ongoing eruptions. For example, a satellite infrared sensor detected the May 18 1980 lateral blast at Mount St. Helens and provided key information on the PDC front velocity¹⁶². However, satellite coverage rarely has sufficient temporal resolution to record the evolution of a phenomenon that, in most cases, lasts only minutes. As a result, ground-based techniques, such as infrasound or Doppler radar, are usually preferred.

PDCs generate acoustic and infrasound waves in the atmosphere and seismic waves in the solid earth ^{163–169}. Infrasound and seismic signals have both been used to detect and locate PDCs and estimate their velocities ^{59,163}. However, the limited spatial resolution of acoustic, seismic and infrasound measurements means that their signals are currently interpreted through conceptual models of the potential PDC structure, rather than validating or refining such conceptions. The main challenge to quantitatively interpreting infrasound and seismic signals is understanding how flow energy is distributed into turbulent fluctuations, by linking the frequency content of the infrasound and seismic signals to dynamic processes of PDC behaviour, its downstream evolution and interactions with natural topography ¹⁶⁶.

The thermal energy content of PDCs influences the air-entrainment rate 152 and buoyancy, and, ultimately, controls the runout and hazard. Information on transport temperatures primarily comes from direct temperature measurements of PDC deposits and thermal proxies preserved in the deposits, such as remnant magnetism^{170,171}, charcoal reflectance^{172,173} and rind thickness on clasts^{174,175}. Direct geophysical measurements using portable thermal infrared cameras have the potential to provide additional, important information about PDC cooling processes associated with the entrainment of ambient air. However, portable thermal cameras need to overcome restrictions associated with the opacity of the gas-particle mixture in infrared wavelengths. As a result, infrared measurements of moving PDCs have, so far, been limited to the detection and tracking of the PDC front176.

Alternatively, probing PDCs with active-source approaches, such as Doppler radar measurements, might provide more information about the interior structure and velocity of the current 177,178. The potential of Doppler

radar has been demonstrated in powder-snow-avalanche research, where microwave radars characterized the internal density stratification of the flow¹⁷⁹. However, a major challenge to radar measurements on active volcanoes is ensuring the equipment has an optimal viewing geometry prior to a PDC event. One study has successfully used Doppler radar to measure the velocity distributions of both dilute and concentrated regimes in a PDC at Colima⁵⁸. Unfortunately, the instrument was destroyed by another sequence of PDCs in 2015, illustrating another major challenge associated with placing valuable geophysical equipment in proximity to active events.

Despite challenges, geophysical measurements offer some of the only means to measure active currents directly, and developing geophysical techniques should be a major focus of future research (FIG. 7a,b). To optimize the insights gained from geophysical measurements of PDCs, their signals must be calibrated experimentally (for example, radar scattering off of different concentrations of volcanic ash). Small-scale and large-scale PDC experiments, as well as numerical calculations, will likely be needed to help interpret geophysical observations.

Video data from large-scale experiments might also help the continued development of optical techniques, such as particle image velocimetry and videogrammetry, to describe turbulent intensity and ash-cloud volume¹⁸⁰. Furthermore, although direct measurements of the internal properties of natural PDCs are very challenging, even a single instrumented measuring site would provide an enormous amount of information to constrain physical and numerical models of PDC transport.

The potential of direct geophysical measurements has been demonstrated in the snow-research community, where powder snow avalanches are artificially triggered and their height-variant and time-variant dynamics probed at a single instrumented site¹⁸¹. As such, direct geophysical measurements of PDCs will provide a driver for future research and a formidable test bench for models, especially when employed for hazard assessment.

PDC hazard modelling

Insights from geophysical measurements, and improved knowledge of the internal dynamics of PDCs, enable increasingly accurate numerical models of PDCs to be created. The main aim of PDC hazard models is to generate forward predictions that can be used, in conjunction with field observations and mapping, to assess and mitigate potential hazards (FIG. 7c-e). The most common approach is to map, in a numerical simulation for a given PDC scenario, the maximum flow dynamic pressure, temperature, in-air particle concentration, the inundation area and the thickness of the deposits Such modelling has multiple challenges, which include uncertainty in the source properties (location, volume, mass flow rate, temperature, duration, grain-size distribution) and boundary conditions (including topography).

There are several key challenges associated with developing a satisfactory model for mapping PDC hazard variables. For example, models must account for a wide range of dynamic scales, flow density stratification, a non-linear granular rheology, broad particle sizes and

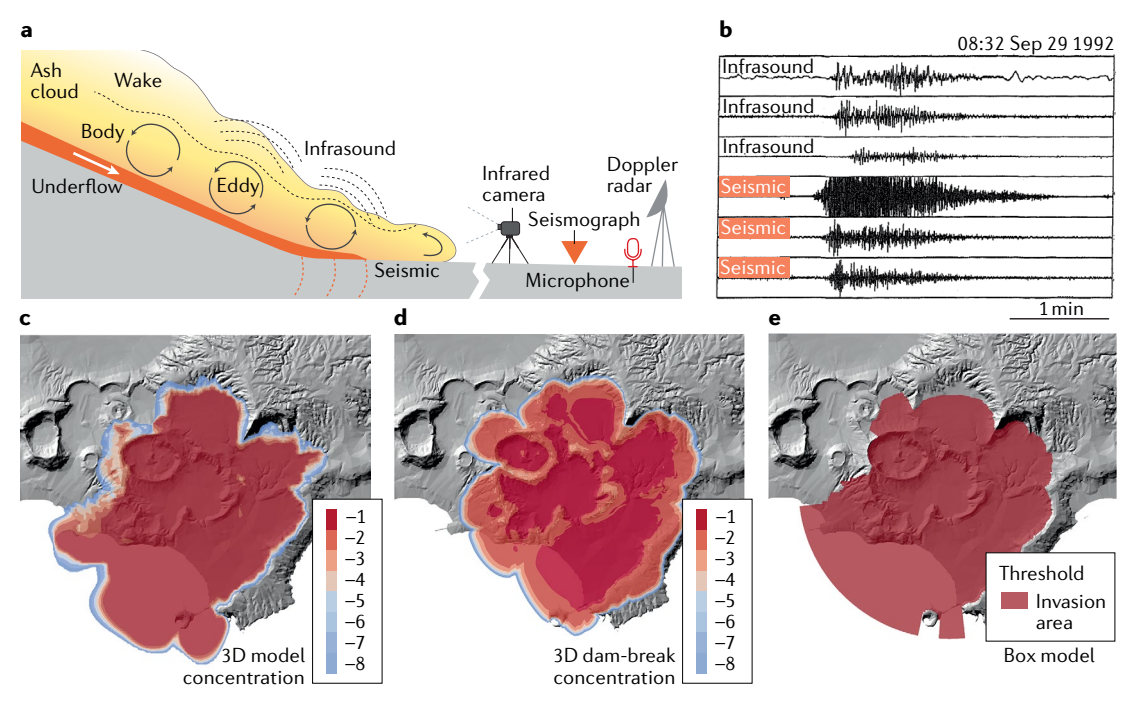


Fig. 7 | Application of geophysical observations and modelling to PDC research. $\bf a$ | A schematic illustration of the possible geophysical measurements, such as infrared imagery and seismic signals, that should be made on real-world pyroclastic density currents (PDCs). Currently, interpretation of geophysical signals is guided by conceptual flow models. $\bf b$ | Infrasound and seismic signals generated by a propagating PDC in 1992 at Mount Unzen (Japan). $\bf c$ | Numerical solution of a 3D model of continuous Plinian-column collapse (mass eruption rate = 10^8 kg s⁻¹, time = 600 s)¹⁹⁸. $\bf d$ | A 3D model of a single collapse impulse (dam break; total mass = 1.6×10^9 kg)¹⁹⁸. $\bf e$ | A calibrated integral box model for a single collapse impulse (total mass = 1.6×10^9 kg)¹⁹⁸. The colour scale in parts $\bf c$ and $\bf d$ represents the particle volume fraction in a logarithmic scale. Variations in the area covered by the PDC models, and their interaction with topography, reflect the initial flow concentration and inertia, and the total mass involved in the PDCs. Part $\bf b$ adapted with permission from REF. ¹⁹³, Japan Meteorological Agency. Parts $\bf c$ and $\bf d$ adapted with permission from REF. ¹⁹⁸, Elsevier.

density distributions, and complex interactions with the substrate and three-dimensional morphology.

Although simplified hazard models with empirically calibrated parameters (such as density stratification and variations in the particle-size distributions) have been developed for other geophysical granular mass flows (such as rock avalanches)^{183,184}, similar empirically calibrated hazard models are currently not available for PDCs. Even in cases where scientists had a relatively broad statistical ensemble of observations to calibrate empirical parameters (such as during the 1995–2010 eruption of Soufrière Hills volcano)¹⁸⁵, hazard prediction has been hindered by three main aspects of volcanic flows.

First, the diversity of PDC generation mechanisms, and the broad range of possible eruption sizes, results in extremely large uncertainties associated with the initial conditions of the flow. Second, frequent unpredictable transitions from concentrated to intermediate or dilute regimes can generate highly mobile turbulent flows, which might decouple from the main current lac, l87. Transitions between regimes and decoupling from the main flow might also occur in response to topographic slope changes, channels and obstacles. Third, the substantial thermal energy contained within PDCs influences internal dynamics and often controls the size of the hazard region. The third point, in particular, is important, since even dilute ash clouds with low dynamic pressure can be lethal at temperatures >100 °C (REF. 188).

Delineating the interaction and separation of concentrated, intermediate and dilute regimes is, therefore, not only a puzzling problem in the theory of granular fluids but also one of the major challenges for modelling PDC hazards^{15,189}. For example, mesoscale clustering in the intermediate regime can enhance sedimentation and modify concentration and temperature stratification, ultimately controlling the dynamic pressure and heat-transfer capacity of a PDC. Therefore, fully accounting for the broad range of recognized gas-particle feedback mechanisms operating within dilute, intermediate and concentrated transport regimes, and including appropriate rheological models that capture the effects of pore-pressure feedback mechanisms on flow mobility, constitute major challenges for future PDC flow models.

Accounting for gas-particle feedback mechanisms is especially important when models are used to assess hazards and support decision-making for risk mitigation and volcanic-crisis management. In such cases, uncertainties in the initial and boundary conditions, as well as uncertainties associated with the flow dynamics, gas-particle feedbacks and other internal PDC processes, should be quantified and managed in a probabilistic framework. However, owing to their high computational costs, two-dimensional and three-dimensional multiphase flow models^{45,152}, which can effectively describe PDC generation and coexistence of the three different flow regimes for single-scenario simulations^{43,112},

are non-optimal for use in a probabilistic framework. Furthermore, there is a developing general consensus that depth-averaged models^{190–196}, which are computationally simple, cannot provide a comprehensive view on all PDC regimes^{64,197}.

One possible compromise is application of multilayered models, in which PDC stratification is simplified into a concentrated, basal layer underlying a dilute ash cloud. In a multilayered model, mass, momentum and energy exchange in the intermediate regime between the two layers can be described by empirical models 190–194. However, to obtain reliable predictions of flow behaviour from a multilayered model, calibration of empirical models in a multilayer formulation is essential (for example, constraining the fluxes of mass, momentum and energy within and through the boundaries of the dilute, intermediate and concentrated regimes).

As such, an emerging method of modelling PDC dynamics that might be particularly useful for probabilistic hazard assessments involves the calibration of low-dimensional models with two-dimensional and three-dimensional numerical simulations. Calibration of low-dimensional models by higher-dimensional models could incorporate complex features of PDCs, such as the deposition and erosion rates at the lower flow boundary, particle sedimentation and elutriation rates from the dilute ash cloud and concentrated basal layer, and the atmospheric air-entrainment rate. For example, FIG. 7e displays a calibrated integral (0D) model, where the effects of topographic barriers on PDC invasion at Campi Flegrei (Italy) are computed by using 3D models (FIG. 7c,d) with different boundary and initial conditions (steady fountaining and single collapse)198. Although simplified models can be calibrated to fit complex model results, input and boundary conditions, the universality of the calibrated parameters (the ability of models calibrated for a particular PDC scenario to produce meaningful results in non-calibrated cases) has to be verified.

To address the challenge of developing robust and accurate PDC hazard forecasts, a broad international initiative (Validation and Benchmarking of Pyroclastic Density Currents initiative of the International Association of Volcanology and Chemistry of the Earth's Interior) has recently commenced to intercompare existing models and to evaluate their inaccuracies in a broad range of PDC flow conditions. The goal is to develop a consensual view on PDC model validation and benchmarking 199, to identify the optimal approach to hazard modelling and to provide guidance on the applicability of models at different levels of approximation.

Summary and future perspectives

Owing to their multifaceted perils, extreme and poorly mitigable hazard intensities, and high risk exposure in growing and expanding society, PDCs remain one of the greatest volcanic hazards. Recently, the combination of data from field studies, large-scale and benchtop-scale experiments, and theoretical and numerical models, has provided critical new insights into the internal dynamics of PDCs. A holistic approach, considering evidence from multiple subdisciplines in PDC research, is required to address the complex, enduring gaps in understanding

the flow and hazard behaviour of PDCs. Below, we highlight several challenges for future research.

Current granular-fluid rheologies that are used in numerical hazard models are based on simplified monodisperse systems. To achieve reliable and rapid hazard forecasts of the concentrated and intermediate transport regimes in PDCs, granular-fluid rheologies must be derived for polydisperse gas-particle mixtures and implemented into existing flow models. Polydisperse gas-particle rheologies will need to address microphysical processes, such as particle interactions with small-scale fluid motion (that is, on the size of an individual particle) and the organization of permeability structures inside flows, which are neither resolved nor parameterized in current models.

Fundamental uncertainties exist on how energy fluctuations are generated, transported and dissipated in PDCs, including the modification of coherent turbulence structures owing to the influence of polydisperse particles, clustering and drag changes. As a result, it remains uncertain how, in dilute and intermediate transport regimes, gas-particle turbulence controls the sedimentation rate, associated momentum loss, flow stratification and buoyancy reversal. In addition, it is still unknown how the granular temperature influences the rheology of concentrated flows. Future research into the generation of energy fluctuations would also add important complexity to newly developed multilayer continuum flow models and inform the constitutive equations for mass, momentum and energy transport within and between layers.

Heat is one of the primary killers in PDC disasters. However, the consequence of temperature modifications on the internal energy, viscosity, density and compressibility of flows and, subsequently, on flow resistance, entrainment and large-scale thermal flow evolution, are poorly understood. Therefore, future laboratory and computational experiments considering thermal effects on scales ranging from the largest eddy to the size of individual particles, in combination with careful characterizations of the thermal properties of natural volcanic material, are needed. The design and thermodynamic scaling of such multidisciplinary studies should be guided by, and ultimately validated against, remote or direct geophysical measurements of the development and evolution of thermal stratification in real-world flows.

Analysis of PDC deposits might offer indirect insights into the characteristics and conditions of hazardous PDCs. However, future field studies are required to link time-variant erosion, deposition and bedform development in the lower flow boundary to the unknown characteristics of internal velocity and density stratification and turbulent near-bed boundary stresses in PDCs. Combined large-scale experiments and high-resolution multiphase simulations could add critical complexity and time-dependence to the simplified relationships between deposit properties and the time-averaged vertical structure that are used in turbulent boundary layer and turbulent sedimentation models.

The international community has started to systematically validate computational flow models against measured flow conditions in large-scale experiments¹⁹⁹.

Critical analysis of computational flow models constitutes an important coming of age of PDC research and will define the strengths, weaknesses and limits of current modelling strategies, and test existing models so that they can be deployed confidently for public safety. However, large-scale experiments cannot capture the full complexity of natural flows. Therefore, although it is certainly an ambitious endeavour, we feel that the strongest scientific advance in PDC research would result from a multinational and multi-instrument effort to measure the internal properties of real-world PDCs to test and advance experiment-based and theory-based knowledge.

Geophysical measurements of the vertical PDC structure, including velocity, density and temperature

fluctuations, and its evolution over natural topography, should be guided by approaches currently utilized in the research of snow avalanches and turbidity currents¹⁸¹. Recent advances in remote and direct geophysical measurement techniques should be used to consider the diversity of PDC behaviour resulting from the natural spectra of flow magnitudes and initiation mechanisms. The resulting data would not only inform realistic model benchmarks but would also provide a more complete picture of the range of multiscale and multiphase processes operating inside PDCs across dilute, intermediate and concentrated flow regime boundaries.

Published online: 30 June 2020

- Dufek, J. The fluid mechanics of pyroclastic density currents. Annu. Rev. Fluid Mech. 48, 459–485 (2016).
 - A review of experimental, theoretical and computational work, with a focus on fluid-dynamic approaches, illustrating advances and current challenges in PDC research.
- Trolese, M., Cerminara, M., Esposti Ongaro, T. & Giordano, C. The footprint of column collapse regimes on pyroclastic flow temperatures and plume heights. Nat. Commun. 10, 2476 (2019).
- Clarke, A. B., Voight, B., Neri, A. & Macedonio, G Transient dynamics of vulcanian explosions and column collapse. *Nature* 415, 897–901 (2002).
- Fink, J. H. & Kieffer, S. W. Estimate of pyroclastic flow velocities resulting from explosive decompression of lava domes. *Nature* 363, 612–615 (1993).
- Cole, P. D. et al. Pyroclastic flows generated by gravitational instability of the 1996–97 lava dome of Soufriere Hills Volcano, Montserrat. Geophys. Res. Lett. 25, 3425–3428 (1998).
- Belousov, A., Voight, B. & Belousova, M. Directed blasts and blast-generated pyroclastic density currents: a comparison of the Bezymianny 1956, Mount St Helens 1980, and Soufriere Hills, Montserrat 1997 eruptions and deposits. *Bull. Volcanol.* 69, 701–740 (2007).
- Komorowski, J.-C. et al. Paroxysmal dome explosion during the Merapi 2010 eruption: processes and facies relationships of associated high-energy pyroclastic density currents. J. Volcanol. Geotherm. Res. 261, 260–294 (2013).
 - Local topographic features can change the internal structure of PDCs and their deposits, dramatically increasing their runout and causing unexpected decoupling of high-energy currents.
- Lube, G. et al. Dynamics of surges generated by hydrothermal blasts during the 6 August 2012 Te Maari eruption, Mt. Tongariro, New Zealand. J. Volcanol. Geotherm. Res. 286, 348–366 (2014). Even small-volume, relatively dilute PDCs can severely impact the volcano surroundings and pose serious hazards for residents and tourists.
- Fujinawa, A., Ban, M., Ohba, T., Kontani, K. & Miura, K. Characterization of low-temperature pyroclastic surges that occurred in the northeastern Japan arc during the late 19th century. J. Volcanol. Geotherm. Res. 178, 113–130 (2008).
- Kaneko, T., Maeno, F. & Nakada, S. 2014 Mount Ontake eruption: characteristics of the phreatic eruption as inferred from aerial observations. Earth Planets Space 68, 72 (2016).
- Lube, G., Cronin, S. J. & Procter, J. N. Explaining the extreme mobility of volcanic ice-slurry flows, Ruapehu volcano, New Zealand. *Geology* 37, 15–18 (2009).
- Self, S. & Rampino, M. R. The 1883 eruption of Krakatau. *Nature* 294, 699–704 (1981).
- Walker, G. P. L., Heming, R. F. & Wilson, C. J. N. Low-aspect ratio ignimbrites. *Nature* 283, 286–287 (1980).
- Baxter, P. J. et al. The impacts of pyroclastic surges on buildings at the eruption of the Soufriere Hills volcano, Montserrat. *Bull. Volcanol.* 67, 292–313 (2005).
- Neri, A., Esposti Ongaro, T., Voight, B. & Widiwijayanti, C. in Volcanic Hazards, Risks and Disasters (eds Shroder, J. F. & Papale, P.) 109–140 (Elsevier, 2015).

- Moore, J. G., & Sisson, T. W. in The 1980 Eruptions of Mount St. Helens, Washington (eds Lipman, P. W. & Mullineaux, D. R.) 421–438 (US Geological Survey, 1981).
- Cronin, S. J. et al. Insights into the October– November 2010 Gunung Merapi eruption (Central Java, Indonesia) from the stratigraphy, volume and characteristics of its pyroclastic deposits. J. Volcanol. Geotherm. Res. 261, 244–259 (2013).
- Valentine, G. A. Damage to structures by pyroclastic flows and surges, inferred from nuclear weapons effects. J. Volcanol. Geotherm. Res. 87, 117–140 (1998).
- Clarke, A. B. & Voight, B. Pyroclastic current dynamic pressure from aerodynamics of tree or pole blow-down. J. Volcanol. Geotherm. Res. 100, 395–412 (2000).
- Jenkins, S. et al. The Merapi 2010 eruption: an interdisciplinary impact assessment methodology for studying pyroclastic density current dynamics.
 J. Volcanol. Geotherm. Res. 261, 316–329 (2013).

 Mastrolorenzo, G. et al. Herculaneum victims of
- Vesuvius in AD 79. *Nature* **410**, 769–770 (2001).
- Baxter, P. J., Neri, A. & Todesco, M. Physical modelling and human survival in pyroclastic flows. *Nat. Hazards* 17, 163–176 (1998).
- Surono et al. The 2010 explosive eruption of Java's Merapi volcano — A '100-year' event. J. Volcanol. Geotherm. Res. 241–242, 121–135 (2012).
- Andreastuti, S. et al. Character of community response to volcanic crises at Sinabung and Kelud volcanoes.
 I. Volcanol. Geotherm. Res. 382, 298–310 (2019)
- Gunawan, H. et al. Overview of the eruptions of Sinabung Volcano, 2010 and 2013–present and details of the 2013 phreatomagmatic phase. J. Volcanol. Geotherm. Res. 382, 103–119 (2019).
- Berger, P. Report on Sinabung (Indonesia). Bulletin of the Global Volcanism Network, 42:2. (ed. Venzke, E.) (Smithsonian Institution, 2017).
- World Bank. Forensic analysis of the conditions of disaster risk in the 2018 Volcano of Fire (Volcán de Fuego) eruption: opportunities for the strengthening of disaster risk management in Guatemala (World Bank Group, 2018).
- Pallister, J. S. et al. Merapi 2010 eruption Chronology and extrusion rates monitored with satellite radar and used in eruption forecasting. J. Volcanol. Geotherm. Res. 261, 144–152 (2013).
- Auker, M. R., Sparks, R. S. J., Siebert, L., Crosweller, H. S. & Ewert, J. A statistical analysis of the global historical volcanic fatalities record. *J. Appl. Volcanol.* 2, 2 (2013).
- Small, C. & Naumann, T. The global distribution of human population and recent volcanism. *Glob. Environ. Change Part B Environ. Hazards* 3, 93–109 (2001).
- Chester, D. K., Degg, M., Duncan, A. M. & Guest, J. E. The increasing exposure of cities to the effects of volcanic eruptions: a global survey. *Clob. Environ. Change Part B Environ. Hazards* 2, 89–103 (2000).
- Branney, M. J. & Kokelaar, P. Pyroclastic Density Currents and the Sedimentation of Ignimbrites Vol. 27 (Geological Society of London, 2002).
- 33. Andrews, B. J. & Manga, M. Experimental study of turbulence, sedimentation, and coignimbrite mass partitioning in dilute pyroclastic density currents. J. Volcanol. Geotherm. Res. 225–226, 30–44 (2012). Laboratory experiments of dilute currents illustrate that turbulence plays a fundamental role in the stratification process of PDCs and their buoyancy reversal.

- Breard, E. et al. Coupling of turbulent and non-turbulent flow regimes within pyroclastic density currents. *Nat. Geosci.* 9, 767–771 (2016).
- Dellino, P. et al. Large-scale experiments on the mechanics of pyroclastic flows: design, engineering, and first results. J. Geophys. Res. Solid Earth 112, B04202 (2007).
- Roche, O. Depositional processes and gas pore pressure in pyroclastic flows: an experimental perspective. *Bull. Volcanol.* 74, 1807–1820 (2012).
 - Experiments illustrate the role of gas pore pressure in reducing friction and modulating the runout distance of PDCs.
- Girolami, L., Druitt, T. H., Roche, O. & Khrabrykh, Z. Propagation and hindered settling of laboratory ash flows. J. Geophys. Res. Solid Earth 113, B02202 (2008).
- Choux, C. M., Druitt, T. H. & Anonymous. Analogue Study of Particle Transport and Sedimentation in Pyroclastic Density Currents (Institut de Physique du Globe de Paris, 2002).
- Brown, R. J. & Andrews, G. D. M. in *The Encyclopedia of Volcanoes* 2nd edn (ed. Sigurdsson H.) 631–648 (Academic, 2015).
- Rowley, P. J., Roche, O., Druitt, T. H. & Cas, R. Experimental study of dense pyroclastic density currents using sustained, gas-fluidized granular flows. *Bull. Volcanol.* 76, 855 (2014).
- Girolami, L., Druitt, T. H. & Roche, O. Towards a quantitative understanding of pyroclastic flows: effects of expansion on the dynamics of laboratory fluidized granular flows. *J. Volcanol. Geotherm. Res.* 296, 31–39 (2015).
- Freundt, A. Formation of high-grade ignimbrites Part II. A pyroclastic suspension current model with implications also for low-grade ignimbrites. Bull. Volcanol. 60, 545–567 (1999).
- Doronzo, D. M., de Tullio, M. D., Dellino, P. & Pascazio, G. Numerical simulation of pyroclastic density currents using locally refined Cartesian grids. Comput. Fluids 44, 56–67 (2011).
- Dufek, J. & Manga, M. In situ production of ash in pyroclastic flows. J. Geophys. Res. Solid Earth 113, B09207 (2008)
- - Three-dimensional, multiphase flow numerical models illuminate several aspects of PDC generation and emplacement, and inform interpretation of PDC deposits.
- Esposti Ongaro, T., Widiwijayanti, C., Clarke, A. B., Voight, B. & Neri, A. Multiphase-flow numerical modeling of the 18 May 1980 lateral blast at Mount St. Helens, USA. Geology 39, 535–538 (2011).
- Fisher, R. V. Transport and deposition of a pyroclastic surge across an area of high relief; the 18 May 1980 eruption of Mount St. Helens, Washington. Geol. Soc. Am. Bull. 102, 1038–1054 (1990).
- Brand, B. D. et al. A combined field and numerical approach to understanding dilute pyroclastic density current dynamics and hazard potential: Auckland Volcanic Field, New Zealand. J. Volcanol. Geotherm. Res. 276, 215–232 (2014).

REVIEWS

- Scott, W. E. et al. in Fire and Mud: Eruptions and Lahars of Mount Pinatubo, Philippines (eds Newhall, C. G. & Punongbayan, R. S.) 545–570 (Univ. Washington Press, 1996).
- Calder, E. S. et al. Mobility of pyroclastic flows and surges at the Soufriere Hills Volcano, Montserrat. Geophys. Res. Lett. 26, 537–540 (1999).
- Druitt, T. H. et al. Small-volume, highly mobile pyroclastic flows formed by rapid sedimentation from pyroclastic surges at Soufriere Hills Volcano, Montserrat; an important volcanic hazard. Geol. Soc. Lond. Mem. 21, 263–279 (2002).
- Loughlin, S. C. et al. Pyroclastic flows and surges generated by the 25 June 1997 dome collapse, Soufriere Hills Volcano, Montserrat. *Geol. Soc. Lond. Mem.* 21, 191–209 (2002).
 Lube, G., Cronin, S. J., Thouret, J.-C. & Surono
- Lube, G., Cronin, S. J., Thouret, J.-C. & Surono Kinematic characteristics of pyroclastic density currents at Merapi and controls on their avulsion from natural and engineered channels. *Geol. Soc. Am. Bull.* 123, 1127–1140 (2011).
- Trolese, M. et al. Very rapid cooling of the energetic pyroclastic density currents associated with the 5 November 2010 Merapi eruption (Indonesia). J. Volcanol. Geotherm. Res. 358, 1–12 (2018).
- Dufek, J., Esposti Ongaro, T. & Roche, O. in *The Encyclopedia of Volcanoes* 2nd edn (ed. Sigurdsson H.) 617–629 (Academic. 2015).
- Breard, E. C. P. & Lube, G. Inside pyroclastic density currents uncovering the enigmatic flow structure and transport behaviour in large-scale experiments. *Earth Planet. Sci. Lett.* 458, 22–36 (2017).
 Large-scale experiments are the only way to reproduce stratified PDCs displaying both concentrated and turbulent behaviour, and to observe the dynamic interaction and continuous transformation between the transport and depositional systems.
 Andrews, B. J. & Manga, M. Effects of topography
- Andrews, B. J. & Manga, M. Effects of topography on pyroclastic density current runout and formation of coignimbrites. *Geology* 39, 1099–1102 (2011).
- Scharff, L., Hort, M. & Varley, N. R. First in-situ observation of a moving natural pyroclastic density current using Doppler radar. Sci. Rep. 9, 7386 (2019).
- Ripepé, M., De Angelis, S., Lacanna, G. & Voight, B. Observation of infrasonic and gravity waves at Soufrière Hills Volcano, Montserrat. *Geophys. Res. Lett.* 37, L00E14 (2010).
- Capra, L. et al. The anatomy of a pyroclastic density current: the 10 July 2015 event at Volcán de Colima (Mexico). Bull. Volcanol. 80, 34 (2018).
- 61. Ogburn, S. E. FlowDat: Mass Flow Database. *Vhub* https://yhub.org/resources/2076 (2013).
- Ogburn, S. E., Loughlin, S. C. & Calder, E. S. DomeHaz: dome-forming eruptions database v2.4. Vhub https://vhub.org/groups/domedatabase (2012).
- Harnett, C. E. et al. Presentation and analysis of a worldwide database for lava dome collapse events: the Global Archive of Dome Instabilities (GLADIS). Bull. Volcanol. 81, 16 (2019).
- Ogburn, S. E. & Calder, E. S. The relative effectiveness of empirical and physical models for simulating the dense undercurrent of pyroclastic flows under different emplacement conditions. Front. Earth Sci. 5, 83 (2017).
- Macorps, E. et al. Stratigraphy, sedimentology and inferred flow dynamics from the July 2015 block-andash flow deposits at Volcán de Colima, Mexico. J. Volcanol. Geotherm. Res. 349, 99–116 (2018).
- Breard, E. C. P., Lube, G., Cronin, S. J. & Valentine, G. A. Transport and deposition processes of the hydrothermal blast of the 6 August 2012 Te Maari eruption, Mt. Tongariro. Bull. Volcanol. 77, 100 (2015).
 Efford, J. T. et al. Vegetation dieback as a proxy for
- Efford, J. T. et al. Vegetation dieback as a proxy for temperature within a wet pyroclastic density current: a novel experiment and observations from the 6th of August 2012 Tongariro eruption. J. Volcanol. Geotherm. Res. 286, 367–372 (2014).
- Pensa, A., Capra, L. & Giordano, G. Ash clouds temperature estimation. Implication on dilute and concentrated PDCs coupling and topography confinement. Sci. Rep. 9, 5657 (2019).
- Wibowo, H. E., Purnama Edra, A., Harijoko, A. & Anggara, F. Emplacement temperature of the overbank and dilute-detached pyroclastic density currents of Merapi 5 November 2010 events using reflectance analysis of associated charcoal. *J. Appl. Geol.* 3, 41–51 (2018).
 Maeno, F. et al. Reconstruction of a phreatic eruption
- Maeno, F. et al. Reconstruction of a phreatic eruption on 27 September 2014 at Ontake volcano, central Japan, based on proximal pyroclastic density current

- and fallout deposits. *Earth Planets Space* **68**, 82 (2016). Fisher, R. V. Models of pyroclastic surges and
- Fisher, R. V. Models of pyroclastic surges and pyroclastic flows. J. Volcanol. Geotherm. Res. 6, 305–318 (1979).
- Fisher, R. V. & Schmincke, H.-U. Pyroclastic Rocks (Springer, 1984).
- Sparks, R. S. J. & Walker, G. P. L. The ground surge deposit: a third type of pyroclastic rock. *Nature* 241, 62–64 (1973).
- Wohletz, K. H. in From Magma to Tephra (eds Freundt, A. & Rosi, M.) 247–312 (Elsevier, 1998).
 Douillet, G. A. et al. Dune bedforms produced by
- Douillet, G. A. et al. Dune bedforms produced by dilute pyroclastic density currents from the August 2006 eruption of Tungurahua volcano, Ecuador. Bull. Volcanol. 75, 1–20 (2013).
- Douillet, G. A. et al. Saltation threshold for pyroclasts at various bedslopes: wind tunnel measurements.
 J. Volcanol. Geotherm. Res. 278–279, 14–24 (2014).
- Sulpizio, R., Mele, D., Dellino, P. & La Volpe, L. Deposits and physical properties of pyroclastic density currents during complex Subplinian eruptions: the AD 472 (Pollena) eruption of Somma-Vesuvius, Italy. Sedimentology 54, 607–635 (2007).
- Brand, B. D. et al. Dynamics of pyroclastic density currents; conditions that promote substrate erosion and self-channelization; mount St Helens, Washington (USA). J. Volcanol. Geotherm. Res. 276, 189–214 (2014).
- Yamamoto, T., Takarada, S. & Suto, S. Pyroclastic flows from the 1991 eruption of Unzen Volcano, Japan. Bull. Volcanol. 55, 166–175 (1993).
- Miyabuchi, Y. Deposits associated with the 1990–1995 eruption of Unzen volcano, Japan. J. Volcanol. Geotherm. Res. 89, 139–158 (1999)
- Wilson, C. J. N. The role of fluidization in the emplacement of pyroclastic flows: an experimental approach. *J. Volcanol. Geotherm. Res.* 8, 231–249 (1980).
- Esposti Ongaro, T., Clarke, A. B., Neri, A., Voight, B. & Widiwijayanti, C. Fluid dynamics of the 1997 Boxing Day volcanic blast on Montserrat, West Indies. J. Geophys. Res. Solid Earth 113, B03211 (2008).
 Lube, G. et al. Flow and deposition of pyroclastic
- Lube, G. et al. Flow and deposition of pyroclastic granular flows: a type example from the 1975 Ngauruhoe eruption, New Zealand. J. Volcanol. Geotherm. Res. 161, 165–186 (2007).
- Geotherm. Res. **161**, 165–186 (2007).

 84. Sheridan, M. F. Emplacement of pyroclastic flows: a review. Geol. Soc. Am. **180**, 125–136 (1979).
- Valentine, G. A. Stratified flow in pyroclastic surges. Bull. Volcanol. 49, 616–630 (1987).
- Druitt, T. Emplacement of the 18 May 1980, lateral blast deposit ENE of Mount St. Helens, Washington. Bull. Volcanol. 54, 554–572 (1992).
- Dellino, P., Mele, D., Sulpizio, R., La Volpe, L. & Braia, G. A method for the calculation of the impact parameters of dilute pyroclastic density currents based on deposit particle characteristics. *J. Geophys. Res. Solid Earth* 113, B07206 (2008).
- Dioguardi, F. & Mele, D. PYFLOW_2.0: a computer program for calculating flow properties and impact parameters of past dilute pyroclastic density currents based on field data. *Bull. Volcanol.* 80, 28 (2018).
- Mele, D. et al. Hazard of pyroclastic density currents at the Campi Flegrei Caldera (Southern Italy) as deduced from the combined use of facies architecture, physical modeling and statistics of the impact parameters. J. Volcanol. Geotherm. Res. 299, 35–53 (2015).
- Burgisser, A. Physical volcanology of the 2,050 BP caldera-forming eruption of Okmok volcano, Alaska Bull. Volcanol. 67, 497–525 (2005).
- Burgisser, A. & Bergantz, G. W. Reconciling pyroclastic flow and surge: the multiphase physics of pyroclastic density currents. Earth Planet. Sci. Lett. 202, 405–418 (2002).
 - Analysis of gas–particle and particle–particle interactions allows a better classification of PDC dynamics in terms of their scaling properties.
- 92. Pope, S. B. *Turbulent Flows* (Cambridge Univ. Press, 2000).
- Gardner, J. E., Nazworth, C., Helper, M. A. & Andrews, B. J. Inferring the nature of pyroclastic density currents from tree damage: The 18 May 1980 blast surge of Mount St. Helens, USA. *Geology* 46, 795–798 (2018).
- Rowley, P. J., Kokelaar, P., Menzies, M. & Waltham, D. Shear-derived mixing in dense granular flows. J. Sediment. Res. 81, 874–884 (2011).
- Ciamarra, M. P., Coniglio, A. & Nicodemi, M. Shear instabilities in granular mixtures. *Phys. Rev. Lett.* 94, 188001 (2005).

- Goldfarb, D. J., Glasser, B. J. & Shinbrot, T. Shear instabilities in granular flows. *Nature* 415, 302–305 (2002)
- Pollock, N. M., Brand, B. D., Rowley, P. J., Sarocchi, D. & Sulpizio, R. Inferring pyroclastic density current flow conditions using syn-depositional sedimentary structures. *Bull. Volcanol.* 81, 46 (2019).
 Roche, O. et al. Dynamic pore-pressure variations
- Roche, O. et al. Dynamic pore-pressure variations induce substrate erosion by pyroclastic flows. *Geology* 41, 1107–1110 (2013).
- Buesch, D. C. Incorporation and redistribution of locally derived lithic fragments within a pyroclastic flow. Geol. Soc. Am. Bull. 104, 1193–1207 (1997)
- Roche, O., Buesch, D. C. & Valentine, G. A. Slow-moving and far-travelled dense pyroclastic flows during the Peach Spring super-eruption. *Nat. Commun.* 7, 10890 (2016).
- Hoblitt, R. P. Observations of the eruptions of July 22 and August 7, 1980, at Mount St. Helens, Washington (US Geological Survey, 1986).
- Bursik, M. I. & Woods, A. W. The dynamics and thermodynamics of large ash flows. *Bull. Volcanol.* 58, 175–193 (1996).
- 103. Pensa, A., Capra, L., Giordano, G. & Corrado, S. Emplacement temperature estimation of the 2015 dome collapse of Volcán de Colima as key proxy for flow dynamics of confined and unconfined pyroclastic density currents. J. Volcanol. Geotherm. Res. 357, 321–338 (2018).
- 104. Giordano, G. et al. Thermal interactions of the AD79 Vesuvius pyroclastic density currents and their deposits at Villa dei Papiri (Herculaneum archaeological site, Italy). Earth Planet. Sci. Lett. 490, 180–192 (2018).
- 105. Brown, R. J. & Branney, M. J. Internal flow variations and diachronous sedimentation within extensive, sustained, density-stratified pyroclastic density currents flowing down gentle slopes, as revealed by the internal architectures of ignimbrites on Tenerife. *Bull. Volcanol.* 75, 727 (2013).
- 106. Cas, R. A. F. et al. The flow dynamics of an extremely large volume pyroclastic flow, the 2.08-Ma Cerro Galan ignimbrite, NW Argentina, and comparison with other flow types. *Bull. Volcanol.* 73, 1583–1609 (2011).
- 107. Silva Parejas, C., Druitt, T. H., Robin, C., Moreno, H. & Naranjo, J. A. The Holocene Pucon eruption of Volcan Villarrica, Chile; deposit architecture and eruption chronology. *Bull. Volcanol.* 72, 677–692 (2010).
- Sparks, R. S. J. Grain size variations in ignimbrites and implications for the transport of pyroclastic flows. Sedimentology 23, 147–188 (1976).
- 109. Breard, E. C. P., Dufek, J. & Lube, G. Enhanced mobility in concentrated pyroclastic density currents: an examination of a self-fluidization mechanism. *Geophys. Res. Lett.* 45, 654–664 (2017).
 110. Lube, G., Breard, E. C. P., Cronin, S. J. & Jones, J.
- 110. Luoe, G., Breard, E. C. P., Cronin, S. J. & Jones, J. Synthesizing large-scale pyroclastic flows: experimental design, scaling, and first results from PELE. J. Geophys. Res. Solid Earth 120, 1487–1502 (2015).
- Res. Solid Earth 120, 1487–1502 (2015).

 111. Dufek, J. & Bergantz, G. W. Suspended load and bed-load transport of particle-laden gravity currents: the role of particle-bed interaction. Theor. Comput. Fluid Dyn. 21, 119–145 (2007).
- Neri, A. et al. 4D simulation of explosive eruption dynamics at Vesuvius. *Geophys. Res. Lett.* 34, 28597 (2007).
- Dellino, P. et al. Experimental evidence links volcanic particle characteristics to pyroclastic flow hazard. Earth Planet. Sci. Lett. 295, 314–320 (2010).
- 114. Andrews, B. J. Dispersal and air entrainment in unconfined dilute pyroclastic density currents. *Bull. Volcanol.* 76, 852 (2014).
- 115. Rodriguez-Sedano, L. A. et al. Influence of particle density on flow behavior and deposit architecture of concentrated pyroclastic density currents over a break in slope: Insights from laboratory experiments. J. Volcanol. Geotherm. Res. 328, 178–186 (2016).
- Douillet, G. A. et al. Pyroclastic dune bedforms: macroscale structures and lateral variations. Examples from the 2006 pyroclastic currents at Tungurahua (Ecuador). Sedimentology 66, 1531–1559 (2019).
- 117. Elghobashi, S. On predicting particle-laden turbulent flows. *Appl. Sci. Res.* **52**, 309–329 (1994).
- 118. Carrara, A., Burgisser, A. & Bergantz, G. W. Lubrication effects on magmatic mush dynamics. *J. Volcanol. Geotherm. Res.* 380, 19–30 (2019)
- J. Volcanol. Geotherm. Res. **380**, 19–30 (2019).

 119. Crowe, C. T., Schwarzkopf, J. D., Sommerfeld, M. & Tsuji, Y. Multiphase Flows with Droplets and Particles (CRC, 2012).

- Weit, A., Roche, O., Dubois, T. & Manga, M. Maximum solid phase concentration in geophysical turbulent gas-particle flows: insights from laboratory experiments. *Geophys. Res. Lett.* 46, 6388–6396 (2019).
- 121. Chen, C. Investigations on Mesoscale Structure in Gas-Solid Fluidization and Heterogeneous Drag Model. Thesis, Tsinghua Univ. (2016).
 122. Chen, C., Li, F. & Qi, H. Modeling of the flue gas
- 122. Chen, C., Li, F. & Qi, H. Modeling of the flue gas desulfurization in a CFB riser using the Eulerian approach with heterogeneous drag coefficient. *Chem. Eng. Sci.* 69, 659–668 (2012).
 123. Wang, W. & Chen, Y. in *Advances in Chemical*
- 123. Wang, W. & Chen, Y. in Advances in Chemical Engineering Vol. 47 (eds Marin, G. B. & Li, J.) 193–277 (Academic, 2015).
- 124. Stix, J. Flow evolution of experimental gravity currents: implications for pyroclastic flows at volcanoes. J. Geol. 109, 381–398 (2001).
- 125. Mangeney, A. et al. Erosion and mobility in granular collapse over sloping beds. *J. Geophys. Res. Earth Surf.* 115, F03040 (2010).
- Pouliquen, O. & Vallance, J. W. Segregation induced instabilities of granular fronts. *Chaos* 9, 621–630 (1999).
- 127. Girolami, L., Roche, O., Druitt, T. H. & Corpetti, T. Particle velocity fields and depositional processes in laboratory ash flows, with implications for the sedimentation of dense pyroclastic flows. Bull. Volcanol. 72, 747–759 (2010).
- 128. Smith, C. M., Williams, R., Rowley, P. J. & Parsons, D. R. Investigation of variable aeration of monodisperse mixtures: implications for pyroclastic density currents. *Bull. Volcanol.* 80, 67 (2018).
- 129. Sulpizio, R., Dellino, P., Doronzo, D. M. & Sarocchi, D. Pyroclastic density currents: state of the art and perspectives. J. Volcanol. Geotherm. Res. 283, 36–65 (2014).
- Cassar, C., Nicolas, M. & Pouliquen, O. Submarine granular flows down inclined planes. *Phys. Fluids* 17, 103301 (2005).
- Breard, E. C. P. et al. The permeability of volcanic mixtures—implications for pyroclastic currents. J. Geophys. Res. Solid Earth 124, 1343–1360 (2019)
- 132. Li, L. & Ma, W. Experimental study on the effective particle diameter of a packed bed with non-spherical particles. *Transp. Porous Media* 89, 35–48 (2011).
- 133. Carman, P. C. Fluid flow through granular beds.
- Chem. Eng. Res. Des. **75**, S32–S48 (1997). 134. Lube, G. et al. Generation of air lubrication within pyroclastic density currents. *Nat. Geosci.* **12**, 381–386 (2019).
- Cole, P. D. et al. Deposits from dome-collapse and fountain-collapse pyroclastic flows at Soufriere Hills Volcano, Montserrat. Geol. Soc. Lond. Mem. 21, 231–262 (2002).
- Montserrat, S., Tamburrino, A., Roche, O. & Niño, Y. Pore fluid pressure diffusion in defluidizing granular columns. J. Geophys. Res. Earth Surf. 117, F02034 (2012).
- Druitt, T. H., Bruni, G., Lettieri, P. & Yates, J. G.
 The fluidization behaviour of ignimbrite at high temperature and with mechanical agitation. Geophys. Res. Lett. 31, L02604 (2004).

 Gravina, T., Lirer, L., Marzocchella, A., Petrosino, P.
- 138. Gravina, T., Lirer, L., Marzocchella, A., Petrosino, P. & Salatino, P. Fluidization and attrition of pyroclastic granular solids. *J. Volcanol. Geotherm. Res.* 138, 27–42 (2004).
- 139. Druitt, T. H., Avard, G., Bruni, G., Lettieri, P. & Maez, F. Gas retention in fine-grained pyroclastic flow materials at high temperatures. *Bull. Volcanol.* 69, 881–901 (2007).
- Iverson, R. M. Regulation of landslide motion by dilatancy and pore pressure feedback. *J. Geophys. Res. Earth Surf.* 110, F02015 (2005).
- Chédeville, C. & Roche, O. Autofluidization of collapsing bed of fine particles: implications for the emplacement of pyroclastic flows. *J. Volcanol. Geotherm. Res.* 368, 91–99 (2018).
- 142. Valentine, G. A. & Sweeney, M. R. Compressible flow phenomena at inception of lateral density currents fed by collapsing gas-particle mixtures. *J. Geophys. Res. Solid Earth* 123, 1286–1302 (2018).
- Chedeville, C. & Roche, O. Autofluidization of pyroclastic flows propagating on rough substrates as shown by laboratory experiments. *J. Geophys. Res. Solid Earth* 119, 1764–1776 (2014).
- 144. Chédeville, C. & Roche, O. Influence of slope angle on pore pressure generation and kinematics of pyroclastic flows: insights from laboratory experiments. *Bull. Volcanol.* 77, 96 (2015).
- 145. Delannay, R., Valance, A., Mangeney, A., Roche, O. & Richard, P. Granular and particle-laden flows: from

- laboratory experiments to field observations. *J. Phys. D Appl. Phys.* **50**, 053001 (2017). 146. Calder, E. S., Sparks, R. S. J. & Gardeweg, M. C.
- 146. Calder, E. S., Sparks, R. S. J. & Gardeweg, M. C. Erosion, transport and segregation of pumice and lithic clasts in pyroclastic flows inferred from ignimbrite at Lascar Volcano, Chile. *J. Volcanol. Geotherm. Res.* 104, 201–235 (2000).
- 147. Rouse, H. Modern conceptions of the mechanics of fluid turbulence. *Trans. ASCE* **102**, 463–505 (1937).
- 148. Sher, D. & Woods, A. W. Mixing in continuous gravity currents. *J. Fluid Mech.* **818**, R4 (2017).
- 149. Druitt, T. H. Pyroclastic density currents. Geol. Soc. Lond. Spec. Publ. 145, 145–182 (1998).
- 150. Fauria, K. E., Manga, M. & Chamberlain, M. Effect of particle entrainment on the runout of pyroclastic density currents. *J. Geophys. Res. Solid Earth* 121, 6445–6461 (2016).
- 151. Sher, D. & Woods, A. W. Experiments on mixing in pyroclastic density currents generated from short-lived volcanic explosions. *Earth Planet. Sci. Lett.* 467, 138–148 (2017).
- 152. Benage, M. C., Dufek, J. & Mothes, P. A. Quantifying entrainment in pyroclastic density currents from the Tungurahua eruption, Ecuador: integrating field proxies with numerical simulations. *Geophys. Res. Lett.* 43, 6932–6941 (2016).
- 153. Dellino, P., Dioguardi, F., Doronzo, D. M. & Mele, D. The entrainment rate of non-Boussinesq hazardous geophysical gas-particle flows: an experimental model with application to pyroclastic density currents. *Geophys. Res. Lett.* 46, 12851–12861 (2019).
- 154. Fullmer, W. D. & Hrenya, C. M. The clustering instability in rapid granular and gas-solid flows. Annu. Rev. Fluid Mech. **49**, 485–510 (2017).
- 155. Agrawal, K., Loezos, P. N., Syamlal, M. & Sundaresan, S. The role of meso-scale structures in rapid gas-solid flows. J. Fluid Mech. 445, 151–185 (2001).
- flows. J. Fluid Mech. 445, 151–185 (2001). 156. Goldhirsch, I. & Zanetti, G. Clustering instability in dissipative gases. Phys. Rev. Lett. 70, 1619–1622 (1993)
- 157. Garzó, V. Instabilities in a free granular fluid described by the Enskog equation. *Phys. Rev. E* 72, 021106 (2005).
- 158. Wylie, J. J. & Koch, D. L. Particle clustering due to hydrodynamic interactions. *Phys. Fluids* **12**, 964–970 (2000)
- 159. Kajishima, T. & Takiguchi, S. Interaction between particle clusters and particle-induced turbulence. *Int. J. Heat Fluid Flow* 23, 639–646 (2002).
- Uhlmann, M. & Doychev, T. Sedimentation of a dilute suspension of rigid spheres at intermediate Galileo numbers: the effect of clustering upon the particle motion. *J. Fluid Mech.* **752**, 310–348 (2014).
 Capecelatro, J., Desjardins, O. & Fox, R. O. Numerical
- Capecelatro, J., Desjardins, O. & Fox, R. O. Numerical study of collisional particle dynamics in cluster-induced turbulence. *J. Fluid Mech.* 747, R2 (2014).
- 162. Moore, J. G. & Rice, C. J. in Explosive Volcanism: Inception, Evolution, and Hazards Ch. 10 133–142 (The National Academies Press, 1984).
- 163. Yamasato, H. Quantitative analysis of pyroclastic flows using infrasonic and seismic data at Unzen volcano, Japan. J. Phys. Earth 45, 397–416 (1997).
- 164. Kelfoun, K., Samaniego, P., Palacios, P. & Barba, D. Testing the suitability of frictional behaviour for pyroclastic flow simulation by comparison with a well-constrained eruption at Tungurahua volcano (Ecuador). Bull. Volcanol. 71, 1057–1075 (2009).
- 165. Uhira, K., Yamasato, H. & Takeo, M. Source mechanism of seismic waves excited by pyroclastic flows observed at Unzen volcano, Japan. J. Geophys. Res. Solid Earth 99, 17757–17773 (1994).
- 166. Allstadt, K. E. et al. Seismic and acoustic signatures of surficial mass movements at volcanoes. *J. Volcanol. Geotherm. Res.* 364, 76–106 (2019).
- 167. Delle Donne, D. et al. in *The Eruption of Soufrière Hills Volcano, Montserrat from 2000 to 2010* Vol. 39 (eds Wadge, G., Robertson, R. E. A. & Voight, B.) (Geological Society of London, 2014).
- 168. Zobin, V. M., Plascencia, I., Reyes, G. & Navarro, C. The characteristics of seismic signals produced by lahars and pyroclastic flows: Volcán de Colima, México. J. Volcanol. Geotherm. Res. 179, 157–167 (2009).
- 169. Ripepe, M. et al. Tracking pyroclastic flows at Soufrière Hills volcano. Eos Trans. Am. Geophys. Union 90, 229–230 (2009).
- 170. Rader, E., Geist, D., Geissman, J., Dufek, J. & Harpp, K. Hot clasts and cold blasts: thermal heterogeneity in boiling-over pyroclastic density currents. Geol. Soc. Lond. Spec. Publ. 396, 67–86 (2015)
- 171. Porreca, M. et al. Paleomagnetic evidence for low-temperature emplacement of the phreatomagmatic

- Peperino Albano ignimbrite (Colli Albani volcano, Central Italy). *Bull. Volcanol.* **70**, 877–893 (2008).
- 172. Sawada, Y., Sampei, Y., Hyodo, M., Yagami, T. & Fukue, M. Estimation of emplacement temperatures of pyroclastic flows using H/C ratios of carbonized wood. J. Volcand. Getherm. Res. 106, 1–20 (2000).
- J. Volcanol. Geotherm. Res. 104, 1–20 (2000).

 173. Scott, A. C. & Glasspool, I. J. Charcoal reflectance as a proxy for the emplacement temperature of pyroclastic flow deposits. Geology 33, 589–592 (2005).
- 174. Benage, M. et al. Tying textures of breadcrust bombs to their transport regime and cooling history. J. Volcanol. Geotherm. Res. 274, 92–107 (2014).
- 175. Carter, A. J. & Ramsey, M. S. ASTER-and field-based observations at Bezymianny Volcano: focus on the 11 May 2007 pyroclastic flow deposit. *Remote Sens. Environ.* 113, 2142–2151 (2009).
- 176. Spampinato, L., Calvari, S., Oppenheimer, C. & Boschi, E. Volcano surveillance using infrared cameras. *Earth-Sci. Rev.* 106, 63–91 (2011).
- 177. Voege, M., Hort, M. & Seyfried, R. Monitoring volcano eruptions and lava domes with Doppler radar. *Eos Trans. Am. Geophys. Union* **86**, 537–541 (2005).
 178. Donnadieu, F. in *Doppler Radar Observations-Weather*
- 178. Donnadieu, F. in Doppler Radar Observations-Weathe Radar, Wind Profiler, Ionospheric Radar, and other Advanced Applications (eds Bech, J. & Chau, J. L.) (IntechOpen, 2012).
- 179. Vriend, N. M. et al. High-resolution radar measurements of snow avalanches. *Geophys. Res. Lett.* 40, 727–731 (2013).
- Andrews, B. J. & Gardner, J. E. Turbulent dynamics of the 18 May 1980 Mount St. Helens eruption column. *Geology* 37, 895–898 (2009).
- 181. Sovilla, B., Schaer, M., Kern, M. & Bartelt, P. Impact pressures and flow regimes in dense snow avalanches observed at the Vallée de la Sionne test site. J. Geophys. Res. Earth Surf. 113, F01010 (2008).
- 182. Calder, E., Wagner, K. & Ogburn, S. in Global Volcanic Hazards and Risk (eds Loughlin, S. C., Sparks, S., Brown, S. K., Jenkins, S. F. & Vye-Brown, C.) 335–342 (Cambridge Univ. Press, 2015).
- Christen, M., Kowalski, J. & Bartelt, P. RAMMS: numerical simulation of dense snow avalanches in three-dimensional terrain. *Cold Reg. Sci. Technol.* 63, 1–14 (2010).
- 184. Hungr, O. & McDougall, S. Two numerical models for landslide dynamic analysis. *Comput. Geosci.* 35, 978–992 (2009).
- 185. Kokelaar, B. P. Sétting, chronology and consequences of the eruption of Soufrière Hills Volcano, Montserrat (1995–1999). Geol. Soc. Lond. Mem. 21, 1–43 (2002).
- 186. Fisher, R. V. Decoupling of pyroclastic currents; hazards assessments. J. Volcanol. Geotherm. Res. 66, 257–263 (1995).
 - Describes the PDCs at Unzen, in 1991, that unexpectedly transformed from concentrated granular flows into dilute turbulent currents, with devastating consequences.
- devastating consequences.

 187. Ogburn, S. E., Calder, E. S., Cole, P. D. & Stinton, A. J.

 The effect of topography on ash-cloud surge generation and propagation. *Geol. Soc. Lond. Mem.* **39**, 179–194 (2014).
- Baxter, P. J. et al. Human survival in volcanic eruptions: Thermal injuries in pyroclastic surges, their causes, prognosis and emergency management. *Burns* 43, 1051–1069 (2017).
- 189. Wadge, G. & Aspinall, W. P. A review of volcanic hazard and risk-assessment praxis at the Soufrière Hills Volcano, Montserrat from 1997 to 2011. Geol. Soc. Lond. Mem. 39, 439–456 (2014).
- 190. Doyle, E. E., Hogg, A. J., Mader, H. M. & Sparks, R. S. J. A two-layer model for the evolution and propagation of dense and dilute regions of pyroclastic currents. J. Volcanol. Geotherm. Res. 190, 365–378 (2010).
- 191. Kelfoun, K. et al. Simulation of block-and-ash flows and ash-cloud surges of the 2010 eruption of Merapi volcano with a two-layer model. J. Geophys. Res. Solid Earth 122, 4277–4292 (2017). Multilayer, depth-averaged models represent a promising computational approach to describe,
- in a simple way, the inner structure of PDCs, but still require calibration of the interaction between the concentrated and dilute layer. 192. Kelfoun, K. A two-layer depth-averaged model for
- both the dilute and the concentrated parts of pyroclastic currents. *J. Geophys. Res. Solid Earth* **122**, 4293–4311 (2017).
- 193. Shimizu, H. A., Koyaguchi, T. & Suzuki, Y. J. The run-out distance of large-scale pyroclastic density currents: a two-layer depth-averaged model. J. Volcanol. Geotherm. Res. 381, 168–184 (2019).

REVIEWS

- 194. Gueugneau, V., Kelfoun, K. & Druitt, T. Investigation of surge-derived pyroclastic flow formation by numerical modelling of the 25 June 1997 dome collapse at Soufrière Hills Volcano, Montserrat. *Bull. Volcanol.* 81, 25 (2019).
- 195. Kelfoun, K. Suitability of simple rheological laws for the numerical simulation of dense pyroclastic flows and long-runout volcanic avalanches. J. Geophys. Res. 116, B08209 (2011).
- 196. Patra, A. K. et al. Parallel adaptive numerical simulation of dry avalanches over natural terrain. J. Volcanol. Geotherm. Res. 139, 1–21 (2005).
- 197. Charbonnier, S. J. et al. Evaluation of the impact of the 2010 pyroclastic density currents at Merapi Volcano from high-resolution satellite imagery, field investigations and numerical simulations. J. Volcanol. Geotherm. Res. 261, 295–315 (2013).
- Esposti Ongaro, T., Orsucci, S. & Cornolti, F. A fast, calibrated model for pyroclastic density currents kinematics and hazard. J. Volcanol. Geotherm. Res. 327, 257–272 (2016).
- **327**, 257–272 (2016). 199. Valentine, G. A. Preface to the topical collection — pyroclastic current models: benchmarking and validation. *Bull. Volcanol.* **81**, 69 (2019).

- Valentine, G. A., Bonadonna, C., Manzella, I., Clarke, A. & Dellino, P. Large-scale experiments on volcanic processes. *Eos Trans. Am. Geophys. Union* 92, 89–90 (2011).
- 201. Pensa, A., Porreca, M., Corrado, S., Giordano, G. & Cas, R. Calibrating the pTRM and charcoal reflectance (Ro%) methods to determine the emplacement temperature of ignimbrites: fogo A sequence, São Miguel, Azores, Portugal, as a case study. Bull. Volcanol. 77, 18 (2015).

Acknowledgements

This work was supported by the Royal Society of New Zealand Marsden Fund (contract nos. MAU1506 and MAU1902), the National Science Foundation (contract no. EAR 1650382), the New Zealand Ministry of Business, Innovation and Employment's Endeavour Fund (contract no. RTVU1704) and Resilience to Nature's Challenges Science Challenge Fund (GNS-RNC047). We thank Michael Manga for the inspiration and help to create the additional figure, and Ermanno Brosch for assisting in the preparation of the figures.

Author Contributions

G.L., E.C.P.B., T.E.-O. and J.D substantially contributed to the discussion of content and wrote and edited the review article.

B.B. substantially contributed to the discussion of content and edited the article.

Competing interests

The authors declare no competing interests.

Peer review information

Nature Reviews Earth & Environment thanks S. Ogburn, G. Douillet and the other, anonymous, reviewer(s) for their contribution to the peer review of this work.

Publisher's note

Springer Nature remains neutral with regard to jurisdictional claims in published maps and institutional affiliations.

Supplementary information

Supplementary information is available for this paper at https://doi.org/10.1038/s43017-020-0064-8.

RELATED LINKS

DomeHaz: https://vhub.org/groups/domedatabase FlowDat: https://vhub.org/groups/massflowdatabase GLADIS: http://vhub.org/groups/domecollapse

© Springer Nature Limited 2020